Quantum Field Theory on Causal Sets

因果集上的量子场论

Nomaan X

诺曼·X

Contents

目录

Abstract

摘要

We give a broad overview of a construction of a theory for matter on fixed causal set backgrounds. We introduce the Sorkin-Johnston formalism for a free (real) scalar field theory that is applicable to regions of

continuum spacetimes as well as to causal sets. We show examples in the causal set, starting from the construction of Green functions to obtaining unique two-point functions using this formalism. We also mention other approaches that have been explored in constructing dynamics for matter on causal sets, including ideas for interacting theories and fermions.

我们全面概述了固定因果集背景下的物质理论构建方法。我们介绍了适用于连续时空区域与因果集的自由 (实) 标量场理论的索金-约翰斯顿形式体系。我们展示了该形式体系在因果集中的应用实例，从格林函数的构建出发，最终得到唯一的两点函数。我们还提及了目前在构建因果集物质动力学过程中已经探索过的其他方法，包括相互作用理论与费米子的相关思路。

Keywords

关键词

Quantum field theory . Sorkin-Johnston vacuum - Green functions .

量子场论。索金-约翰斯顿真空-格林函数。

Geometric quantization - Causal diamond - Mottola-Allen vacua - Spacetime discreteness . Poisson sprinkling

几何量子化-因果菱形-莫托拉-艾伦真空-时空离散性。泊松喷淋

Nomaan X (☑)

努曼·X(☑)

Department of Mathematics and Statistics, University of New Brunswick, Fredericton, NB, Canada

加拿大新不伦瑞克省弗雷德里克顿新不伦瑞克大学数学与统计系

e-mail: nomaan.math@unb.ca

电子邮箱:nomaan.math@unb.ca

Introduction

引言

The main motivation for wanting to describe QFT on a discrete spacetime background is to avoid divergences (Lattice field theory is the most straightforward but less foundational implementation of this idea with

the advantage of being amenable to numerical/computational methods.). Traditionally, this was handled by a variety of renormalization techniques which, initially introduced as technical tools to obtain sensible results, are now understood in the sense of Wilsonian renormalization as ways of obtaining an effective field theory. The idea being that since we don't know the full UV complete theory, we're always dealing with effective descriptions involving energy-dependent parameters. These effective descriptions stop making sense beyond certain energy scales. This approach has seen stunning success as far as high energy physics phenomenology goes. It has also become the standard way of studying condensed matter systems.

我们希望在离散时空背景下描述量子场论 (QFT) 的核心动机是避免发散 (格点场论是这一思路最直接但基础层面研究较少的实现方式，其优势是适合数值/计算方法处理)。传统上该问题通过多种重整化技术解决: 这些技术最初只是获得合理结果的技术工具，如今在威尔逊重整化的框架下被理解为得到有效场论的方法。核心思路是，由于我们不清楚完整的紫外完备理论，我们始终只能处理包含能量依赖参数的有效描述；这些有效描述在特定能标以上就不再成立。就高能物理唯象学而言，该方法取得了惊人的成功，也已成为研究凝聚态系统的标准方法。

In the study of quantum gravity however, this approach has severe limitations. Firstly, by construction it throws away information on the deep UV regime. Secondly, while the renormalization group flow description of couplings in a theory can indicate the breakdown of effective theories, it will not signal the appearance of radically new physics that may arise. Ideas such as non-locality, stochastic behavior of matter (or gravity), causality violation, and the breakdown of notions tied to the continuum are not trivial extensions of local, renormalizable, continuum-based effective field theories.

但在量子引力研究中，该方法存在严重局限性: 首先，从构造上来说它会丢弃深紫外区域的信息；其次，尽管重整化群流对理论耦合的描述可以指示有效理论的失效，但它无法预示可能出现的全新物理。非局域性、物质 (或引力) 的随机行为、因果性破坏，以及连续统相关概念的失效这类想法，都不是局域、可重整、基于连续统的有效场论的平凡推广。

The interest in studying QFT on causal sets is not only a way around these limitations but is in itself an important ingredient in thinking of causal sets as fundamental to quantum gravity. It is foundational and bottom-up in the same sense as Boltzmann's statistical mechanics was in describing standard macroscopic thermodynamics of his time. Even putting aside the question of whether causal sets are in fact fundamental or not, we might be interested in studying QFT on a discrete background which, unlike say a simple hypercubic lattice, shares basic properties of continuum spacetime (e.g., Lorentzian signature and Lorentz-invariance). Effects of spacetime discreteness from the causal set may show up at larger scales in observations and/or experiments; at the very least, it will help us constrain the discreteness parameters.

研究因果集上量子场论的兴趣，不仅是规避这些局限的一种途径，本身也是将因果集视为量子引力基础理论的重要组成部分。它是基础性的、自下而上的研究，就像玻尔兹曼统计力学描述当时的宏观热力学一样。即使抛开因果集是否真的是基本理论这一问题不谈，我们也有必要研究离散背景上的量子场论——和简单超立方格点不同，因果集保留了连续时空的基本性质 (例如洛伦兹号差和洛伦兹不变性)。因果集带来的时空离散效应可能会在更大尺度的观测和/或实验中显现；至少它能帮助我们约束离散化参数。

Various approaches to studying QFT on causal sets have been considered, and below we provide a brief summary:

学界已经提出了多种研究因果集上量子场论的方法，我们在此做简要总结:

- Matter as a causal set: These are inspired from Wheeler's geometrodynamics where field configurations are encoded in patterns arising from the causal structure, i.e., matter arises from spacetime. An example has been proposed here [27]. Another possibility is to model matter àla Kaluza-Klein, where we start with a higher-dimensional causal set dynamics and try to split this into a lower-dimensional causal set part along with a matter part. This is yet to be implemented.

  - 物质即因果集: 这类研究受惠勒几何动力学启发，将场构型编码在因果结构涌现的模式中，即物质从时空中涌现。文献 [27] 已经提出了一个例子。另一种可能是模仿卡鲁扎-克莱因理论建模物质: 从高维因果集动力学出发，尝试将其拆分为低维因果集部分和物质部分，这一思路尚未实现。

- Matter on a causal set: This is along the lines of standard QFT where dynamics of matter are described on a background spacetime. There have been multiple approaches to this:

  - 因果集上的物质: 这遵循标准量子场论的思路，即在背景时空上描述物质的动力学。这类研究已有多种方法:

1. Scalar field theory in histories form: Histories-based formulations of quantum theories are regarded as more satisfactory than operator formulations for various reasons. Such an approach for a free scalar field on causal sets is based on the decoherence functional $D\left(\zeta,\overline{\zeta}\right)$ that maps pairs of spacetime histories (A pair is called a Schwinger history in honor of the Schwinger-Keldysh version of the path integral.) of the scalar field to complex numbers. The dynamics must then be described in terms of D and a quantum measure obtained from it. Suggestions for generalizations to interacting theory have also been proposed [25].

1. 历史形式的标量场论: 出于多种原因，基于历史的量子理论表述被认为比算符表述更令人满意。因果集上自由标量场的这种方法基于退相干泛函 $D\left(\zeta,\overline{\zeta}\right)$，它将标量场的时空历史对 (为纪念路径积分的施温格-凯尔迪什版本，一对历史被称为施温格历史) 映射为复数。之后动力学必须用 D 和从中得到的量子测度描述。向相互作用理论推广的方案也已被提出 [25]。

2. Green functions and the Sorkin-Johnston formalism: In this approach, the classical equations of motion are bypassed, and we directly identify a retarded Green function for the scalar field. Then, we use the SJ formalism to construct a unique Wightman function for the theory [19, 26]. This approach has been studied the most, not just in the context of causal sets [19, 28] but also in the continuum [2, 20, 26] , where it can be used as an alternative to canonical quantization. Importantly, it provides a way around the problem of the choice of a vacuum in arbitrary spacetime regions.

2. 格林函数与索尔金-约翰斯顿形式化: 该方法绕过了经典运动方程，直接确定标量场的推迟格林函数，之后我们用 SJ 形式化构造该理论唯一的威彻曼函数 [19, 26]。该方法是目前研究最多的，不仅在因果集背景下 [19, 28]，在连续统 [2, 20, 26] 中也可以作为正则量子化的替代方案。重要的是，它解决了任意时空区域中真空选择的问题。

Recently, an alternate way of defining a vacuum state using the notion of geometric quantization instead of using the SJ axioms (see below) has been proposed [16]. This method can be applied to symplectic manifolds

with a Riemannian metric. In the case of causal sets, this means applying the procedure to a symplectic vector space with an inner product, which results in a state identical to the SJ state.

最近，有研究提出了不用 SJ 公理 (见下文)，改用几何量子化概念定义真空态的替代方法 [16]。该方法可应用于带黎曼度量的辛流形。在因果集的情况，这相当于将该过程应用于带内积的辛向量空间，最终得到的态与 SJ 态完全一致。

3. d'Alembertians: A scalar field on continuum spacetime satisfies the Klein-Gordon equation. A natural step in discretization is therefore to find the causal set analog of the d'Alembertian operator. One way to do this is to identify a Green function and then invert it. This was tried in regions of $\mathbb{M}^2$ [10, 23] and found to be a good approximation to the continuum d'Alembertian for fields which vary slowly on the discreteness scale and are zero on the boundary of the region considered.

3. 达朗贝尔算符: 连续时空上的标量场满足克莱因-戈登方程，因此离散化的一个自然步骤就是找到因果集中对应达朗贝尔算符的类比。实现这一点的一种方法是找到格林函数再对其求逆，该方法已在 $\mathbb{M}^2$ [10, 23] 区域中进行了尝试，结果表明，对于在离散尺度上缓慢变化、且在所研究区域边界处为零的场，该方法是连续达朗贝尔算符的良好近似。

Another, better studied way is to construct a d'Alembertian operator in a way analogous to the usual second-order differential operator, as a difference operator using nearest neighbors. However, due to the Lorentzian nature of the metric, it is not obvious how to identify "nearest neighbors." A way around this was the proposal to use a past-layered decomposition of the causal set and then sum over these layers with appropriate coefficients [6,24]. A class of such d'Alembertians has now been constructed for different geometries and dimensions [4, 11].

另一种研究更充分的方法是，类比常规二阶微分算子，利用最近邻构造差分形式的达朗贝尔算符。但由于度规具有洛伦兹特性，如何定义“最近邻”并不明确。针对该问题，一个解决方案是提议对因果集做过去分层分解，再对各层按合适系数求和 [6,24]。目前已经针对不同几何和维度构造了一系列这类达朗贝尔算符 [4, 11]。

It remains an open question as to how these d'Alembertians can be used to define a full field theory on the causal set.

如何用这些达朗贝尔算符定义因果集上的完整场论，目前仍是一个开放问题。

4. Field Lagrangians: This approach is based on re-expressing the classical field Lagrangian in terms of the causal structure, the volume element, and the proper time, i.e., quantities derived from the causal set [29]. While this has the advantage of being amenable to gauge fields and spinors, it is a top-down approach that starts from the continuum and leads to a somewhat complicated causal set expression. Instead, it would be appealing to start from things defined on the causal set and then take the continuum limit as a cross-check.

4. 场拉格朗日量: 该方法的基础是将经典场拉格朗日量重新用因果结构、体积元和固有时——即源自因果集的物理量——来表示 [29]。尽管它的优势是适用于规范场和旋量，但它是一种自上而下的方法: 从连续时空出发，最终得到的因果集表达式相对复杂。反过来，从因果集上定义的量出发，再取连续极限作为交叉检验，会更理想。

We note that while the motivations for constructing QFT on causal sets come from quantum gravity, such a construction, as a UV complete theory would require evaluating the full path integral over all causal sets and field configurations. This is beyond our current understanding of the subject. Instead, we build QFT on sprinkled causal sets, i.e., causal sets approximated by fixed regions of continuum spacetime. This way, we can focus on aspects of quantum fields on causal sets without the complications arising from dynamics of causal sets themselves. This corresponds to working at a mesoscale that is not quite the Planck (or discreteness) scale but incorporates the effects of discreteness. Hence, we probe higher energies than QFT on curved spacetime, which might be phenomenologically relevant.

我们注意到，虽然在因果集上构造量子场论的动机来自量子引力，但这样的构造作为一个紫外完备理论，需要对所有因果集和场构型计算完整路径积分，这超出了我们目前对该领域的理解。因此我们选择在撒播因果集——即由连续时空固定区域近似得到的因果集——上构造量子场论。通过这种方式，我们可以专注于因果集上量子场的相关问题，规避因果集自身动力学带来的复杂性。这对应于在介观尺度开展研究: 该尺度不是严格的普朗克尺度 (或离散尺度)，但已经包含了离散效应。因此我们探究的能标比弯曲时空上的量子场论更高，这可能在唯象学上具有研究价值。

The Sorkin-Johnston Method

索尔金-约翰斯顿方法

The method we describe here is for the construction of a theory of a free (real) scalar field. We also note that this construction can be carried out rigorously in the continuum as well [1, 12, 26] . Here we review the continuum construction and then restrict ourselves to the causal set where the construction is greatly simplified.

我们在此介绍的方法用于构造自由 (实) 标量场理论。需要说明的是，该构造也可以在连续统中严格完成 [1, 12, 26] 。本文我们先回顾连续统构造，再将讨论范围限定在因果集上，该构造在因果集上会得到大幅简化。

We will proceed in an unorthodox manner that is more suited to the causal set - rather than start with the field equations (While there are algebraic conditions that can potentially be used as equations of motion on the causal set, they are not analogous to the dynamical equations that we are used to in standard field theory.) - the construction will be based on the retarded Green function of the field. The two-point correlation function or the Wightman function can then be derived from this Green function:

我们将采用更适配因果集的非传统方式开展推导——不从场方程出发 (尽管存在一些代数条件，它们或可作为因果集上的运动方程，但这些条件并不类似于我们在标准场论中所熟悉的动力学方程)——整个构造将基于场的推迟格林函数。两点关联函数即维特曼函数可由此格林函数推导得出:

$$G \to \Delta \to W \tag{1}$$

where Δ is called the Pauli-Jordan function and we define it below. Such an approach builds in state information from the very beginning, in the form of the Wightman function, $W(x, x')$.

其中 Δ 被称为泡利-若尔当函数，我们会在下文中对其下定义。这种方法从一开始就以维特曼函数的形式内置了态信息 $W(x,x')$ 。

We begin our discussion with the first step in the construction, the identification of appropriate Green functions on the causal set. In general, there is no known way to obtain a Green function starting from the causal set. The examples we discuss below are some known and interesting cases where the Green function on the causal set can be motivated from the knowledge of the corresponding continuum Green function. We will also see that there are usually multiple ways to do this, and we expect that they converge in the continuum limit. Toward the end of the following section, we briefly mention alternate proposals for obtaining Green functions.

我们从构造的第一步开始讨论，即确定因果集上合适的格林函数。一般而言，目前尚无已知方法可以从因果集出发直接得到格林函数。下文我们讨论的例子都是已知的典型情形，在这些情形中，可以借助对应连续统格林函数的已知结论推导出因果集上的格林函数。我们还会看到，通常存在多种实现方式，且我们预期这些方式在连续统极限下会收敛。在下一节的末尾，我们会简要介绍获取格林函数的其他方案。

Green Functions

格林函数

Before we discuss examples of constructing Green functions, we note an important connection between the massless and massive Green functions. Consider the massless scalar retarded Green function $G_0(x,x')$ on a globally hyperbolic d dimensional spacetime (M,g) :

在讨论构造格林函数的例子之前，我们先介绍无质量格林函数与有质量格林函数之间一个重要联系。考虑整体双曲 d 维时空 (M,g) 上的无质量标量推迟格林函数 $G_0(x,x')$:

$$\Box_x G_0(x,x') = -\frac{1}{\sqrt{-g(x')}}\delta(x-x'). \tag{2}$$

The massive retarded Green function, G_m , satisfies:

有质量推迟格林函数 G_m 满足:

$$\left(\Box_x - m^2\right) G_m(x,x') = -\frac{1}{\sqrt{-g(x)}}\delta(x-x'), \tag{3}$$

and can be written as a formal expansion

并且可以写为形式展开

$$G_m = G_0 - m^2 G_0 * G_0 + m^4 G_0 * G_0 * G_0 + \ldots = \sum_{k=0}^{\infty} \left(-m^2\right)^k \underbrace{G_0 * G_0 * \ldots G_0}_{k+1}$$

(4)
where

其中

$$(A * B)(x, x') \equiv \int d^d x_1 \sqrt{-g(x_1)} A(x, x_1) B(x_1, x'). \tag{5}$$

If $G_0(x, x')$ is retarded, then so is $G_m(x, x')$.

若 $G_0(x, x')$ 是推迟格林函数，则 $G_m(x, x')$ 也是推迟格林函数。

Consider the more general case of a scalar theory in curved spacetime. The Green function satisfies:

考虑弯曲时空中标量理论的更一般情形。格林函数满足:

$$\left(\Box_g - m^2 - \xi R\right) G_{m,\xi}(x, x') = \frac{1}{\sqrt{-g(x)}} \delta(x - x'). \tag{6}$$

$G_{m,\xi}(x, x')$ can be obtained from $G_{0,\xi}(x, x')$ using the same series expansion Eq. (4):

$G_{m,\xi}(x, x')$ 可以通过相同的级数展开式 (4) 由 $G_{0,\xi}(x, x')$ 得到:

$$G_{m,\xi} = \sum_{k=0}^{\infty} \left(-m^2\right)^k \underbrace{G_{0,\xi} * G_{0,\xi} * \ldots G_{0,\xi}}_{k+1}. \tag{7}$$

Further, in the special case when R is a constant, the ξR term just modifies the mass, and $G_{m,\xi}(x, x')$ can be obtained from the massless minimally coupled (MMC) Green function $G_{0,0}(x, x')$ with m^2 replaced by $m^2 + \xi R$. In general, for constant R, we can relate the two Green functions:

此外，在 R 为常数的特殊情形下，ξR 项仅对质量做修正，且 $G_{m,\xi}(x, x')$ 可以由将 m^2 替换为 $m^2 + \xi R$ 后的无质量最小耦合 (MMC) 格林函数 $G_{0,0}(x, x')$ 得到。一般而言，当 R 为常数时，我们可以将两个格林函数联系起来:

$$G_{m',\xi'} = \sum_{k=0}^{\infty} \left(-m'^2 - \xi' R + m^2 + \xi R\right)^k \underbrace{G_{m,\xi} * G_{m,\xi} * \ldots G_{m,\xi}}_{k+1}, \tag{8}$$

for any $(m, \xi), (m', \xi')$.

对任意 $(m, \xi), (m', \xi')$ 成立。

Therefore, if we have the massless (or MMC) retarded Green function, we can write down a formal series for the massive retarded Green function. Note that, in the $d = 2$ case, this formal series contains IR divergences in each term due to the presence of G_0 [5]. However, on causal sets the expression is well-defined since we are always working with matrices and finite sums.

因此，如果我们已知无质量 (或最小耦合无质量) 推迟格林函数，就可以写出有质量推迟格林函数的形式级数。注意，在 $d=2$ 情形下，由于 G_0 的存在，该形式级数每一项都包含红外发散 [5]。但在因果集上这个表达式是良定义的，因为我们始终是在矩阵和有限和的框架下计算。

If we have a massless (or MMC) retarded Green function analogue (We avoid writing ξ in the causal set expressions; however, when appropriate, ξ will modify the mass as discussed for the continuum case.), $K_0(x,x')$, on a causal set with sprinkling density ρ in a volume V of d -dimensional spacetime, we can propose a massive retarded Green function $K_m(x,x')$ via the replacement:

如果我们在撒播密度为 ρ 、体积为 V 的 d 维时空因果集上，得到了无质量 (或最小耦合无质量) 推迟格林函数的类比 (我们避免在因果集表达式中写出 ξ ；不过在适用情形下，ξ 会像连续统情形中讨论的那样修正质量) $K_0(x,x')$ ，我们就可以通过下述替换得到有质量推迟格林函数 $K_m(x,x')$:

$$\int \sqrt{-g(x)}d^dx \to \rho^{-1} \sum_{\text{causal set elements}}, \tag{9}$$

leading to

由此得到

$$K_m = \sum_{k=0}^{\infty}\left(-\frac{m^2}{\rho}\right)^k \underbrace{K_0 \cdot K_0 \ldots K_0}_{k+1} \tag{10}$$

where now the convolutions become matrix products. The series terminates and is well-defined for each pair x and x' because, as we will see, the matrices involved in the products are nilpotent.

其中卷积在这里变为矩阵乘积。该级数是截断的，且对任意一对 x 和 x' 都是良定义的，因为我们之后会看到，乘积中涉及的矩阵是幂零矩阵。

The key to the above construction of a massive Green function is knowing the massless one. We can repeat it on causal sets if we can find the appropriate massless retarded Green function analogues for causal sets sprinkled into general curved spacetimes.

上述构造有质量格林函数的关键在于已知无质量格林函数。如果能找到嵌入一般弯曲时空的因果集对应的合适无质量推迟格林函数类比，我们就可以在因果集上重复这个构造。

We now show a few examples of explicit construction of Green functions[19,22].

下面我们给出几个显式构造格林函数的例子 [19,22]。

$d=2$ Minkowski

$d=2$ 闵氏空间

The massless retarded Green function in $d=2$ Minkowski spacetime $\mathbb{M}^2$ is

$d = 2$ 闵氏时空 $\mathbb{M}^2$ 中的无质量推迟格林函数为

$$G_0^{(2)}(x, x') = \frac{1}{2}\theta(x_0 - x_0')\,\theta\left(\tau^2(x, x')\right) \tag{11}$$

where τ is the proper time and θ is the Heaviside step function.

其中 τ 是固有时，θ 是赫维赛德阶跃函数

For any causal set $\mathcal{C}$, we can define a causal matrix $C_0(x, x')$ as

对于任意因果集 $\mathcal{C}$ ，我们可以定义因果矩阵 $C_0(x, x')$ 为

$$C_0(x, x') := \begin{cases} 1 \text{ if } x' \prec x \\ 0 \text{ otherwise} \end{cases}$$

The Poisson sprinkling gives a random variable, which we also call $C_0(x, x')$, for every two points, x and x' on that $\mathcal{C}$. It was shown (This is also intuitively clear from the definition of the causal matrix.) [10] that the average value of this variable is

泊松喷洒为该 $\mathcal{C}$ 上任意两点 x 和 x' 给出了一个随机变量，我们也将其称为 $C_0(x, x')$ 。已有结论证明 (从因果矩阵的定义来看，这在直觉上也是显然的)[10]，该随机变量的平均值为

$$\langle C_0(x, x')\rangle = 2G_0^{(2)}(x, x')\,. \tag{12}$$

This suggests that the causal matrix as the analogue Green function in this case

这表明因果矩阵就是该情形下的类比格林函数

$$K_0^{(2)}(x, x') \equiv \frac{1}{2}C_0(x, x')\,. \tag{13}$$

Then, a massive Green function $K_m^{(2)}(x, x')$ on $\mathcal{C}$ can be defined using this and Eq. (10) as

随后，结合该结论与式 (10)，可以定义 $\mathcal{C}$ 上的有质量格林函数 $K_m^{(2)}(x, x')$ 为

$$K_m^{(2)}(x, x') = \sum_{k=0}^{\infty}\left(-\frac{m^2}{\rho}\right)^k\left(\frac{1}{2}\right)^{k+1}C_k(x, x')\,, \tag{14}$$

where C_k ' s are called k -chains and are powers of the causal matrix - $C_k(x, x') =$

其中 C_k 被称为 k 链，是因果矩阵的幂——即 $C_k(x, x') =$

$\underbrace{C_0 \cdot C_0 \cdot \ldots C_0}_{k+1}(x, x')$.

It can be shown that the average value of the corresponding random variable, for any sprinkling density, is equal to the continuum massive Green function:

可以证明，对任意喷洒密度，对应的随机变量的平均值都等于连续有质量格林函数:

$$\left\langle K_m^{(2)}(x,x')\right\rangle = G_m^{(2)}(x,x')\,. \tag{15}$$

Another way to interpret $K_m^{(2)}(x,x')$ is in terms of hop and stop weights, a and b , respectively [17]:

解释 $K_m^{(2)}(x,x')$ 的另一种方法是通过跳跃权重和停止权重，分别对应 a 和 b ，如文献 [17] 所示:

$$K_m^{(2)}(x,x') = \sum_{k=0}^{\infty} a^{k+1} b^k C_k(x,x')\,. \tag{16}$$

This form is interpreted as a sum over all chains between x and x' : for each k -chain, the hop between two successive elements has weight a , and the stop at each intervening element between x and x' has weight b . We see that the weight $a = 1/2$ is associated with each factor of $K_0^{(2)}$ (from the relationship between $K_0^{(2)}$ and the causal matrix) and the weight $b = -m^2/\rho$ to each convolution. We will see below that in certain spacetimes with curvature, manipulating these weights appropriately will give us the right Green function.

该形式可以解释为对 x 和 x' 之间所有链的求和: 对每条 k 链，两个相邻元素之间的跳跃权重为 a ，x 和 x' 之间每个中间元素的停止权重为 b 。我们可以看到，权重 $a = 1/2$ 对应 $K_0^{(2)}$ 的每个因子 (由 $K_0^{(2)}$ 和因果矩阵的关系可得)，权重 $b = -m^2/\rho$ 对应每次卷积。我们下文将会看到，在某些弯曲时空中，适当调整这些权重即可得到正确的格林函数。

$d = 4$ Minkowski

$d = 4$ 闵可夫斯基

In $d = 4$ Minkowski spacetime, $\mathbb{M}^4$, the retarded Green function for the massless field is

在 $d = 4$ 闵可夫斯基时空中，$\mathbb{M}^4$ ，无质量场的推迟格林函数为

$$G_0^{(4)}(x,x') = \frac{1}{2\pi}\theta(x_0 - x_0')\,\delta\left(\tau^2(x,x')\right), \tag{17}$$

The causal set analogue is proportional to the link matrix defined as

因果集对应形式正比于如下定义的链接矩阵:

$$L_0(x,x') := \begin{cases} 1 \text{ if } x' \prec x \text{ and } |(x,x')| = 0 \\ 0 \text{ otherwise} \end{cases},$$

The average value of the corresponding random variable $L_0(x,x')$ in a Poisson sprinkling of density ρ is

密度为 ρ 的泊松撒播中，对应随机变量 $L_0(x,x')$ 的平均值为

$$\langle L_0(x,x')\rangle = \theta(x_0 - x_0')\,\theta\left(\tau^2(x,x')\right)\exp\left(-\rho V(x,x')\right), \tag{18}$$

where $V(x,x')$ is the volume of the spacetime interval (Such an interval is called a causal diamond or Alexandrov interval.) $J^-(x)\cap J^+(x')$. Using $V(x,x') = \frac{\pi}{24}\tau^4(x,x')$, it can be shown that

其中 $V(x,x')$ 是时空区间 (这类区间称为因果菱形或亚历山德罗夫区间) 的体积 $J^-(x)\cap J^+(x')$。利用 $V(x,x') = \frac{\pi}{24}\tau^4(x,x')$ 可以证明

$$\lim_{\rho\to\infty}\sqrt{\frac{\rho}{6}}\langle L_0(x,x')\rangle = 2\pi G_0^{(4)}(x,x'). \tag{19}$$

This suggests that we pick the massless Green function in this case as

这说明我们在该情形下选取的无质量格林函数为

$$K_0^{(4)}(x,x') = \frac{1}{2\pi}\sqrt{\frac{\rho}{6}}L_0(x,x'). \tag{20}$$

The relationship with the continuum Green function is not as direct here because it is only in the continuum limit as $\rho\to\infty$ that the average value of $K_0^{(4)}$ equals the continuum $G_0^{(4)}$. In Fig. 1 we plot binned and averaged values for the causal set retarded Green function Eq. (20) along with its average value at finite density obtained from Eq. (18) in a causal diamond of height unity. The corresponding continuum Green function Eq. (17) has a delta function on the lightcone and is therefore infinitely sharply peaked there. While this is not the case in the causal set, the discrepancy grows smaller as the density is increased.

它与连续体格林函数的联系在这里没那么直接，因为只有当 $\rho\to\infty$ 取连续极限时，$K_0^{(4)}$ 的平均值才等于连续体的 $G_0^{(4)}$。在图 1 中，我们绘制了高度为 1 的因果菱形里，式 (20) 给出的因果集推迟格林函数的分箱平均取值，以及式 (18) 得到的有限密度下的平均值。对应连续体的式 (17) 格林函数在光锥上存在一个德尔塔函数，因此在该处是无限尖峰的。因果集中不存在这种情况，随着密度增大，二者的差异会逐渐缩小。

We use this $K_0^{(4)}$ to construct a massive Green function $K_m^{(4)}(x,x')$ via Eq. (10) as before:

我们和之前一样，利用这个 $K_0^{(4)}$ 通过式 (10) 构造有质量格林函数 $K_m^{(4)}(x,x')$：

$$K_m^{(4)}(x,x') = \sum_{k=0}^{\infty}\left(-\frac{m^2}{\rho}\right)^k\left(\frac{1}{2\pi}\sqrt{\frac{\rho}{6}}\right)^{k+1}L_k(x,x'). \tag{21}$$

Fig. 1 The binned and averaged plot for K_0 vs. $|\tau|$ (timelike distance) as N is varied. The black curve represents the average value for $N = 31k$

图 1 随 N 变化，K_0 对 $|\tau|$ (类时距离) 的分箱平均图。黑色曲线代表 $N = 31k$ 的平均值

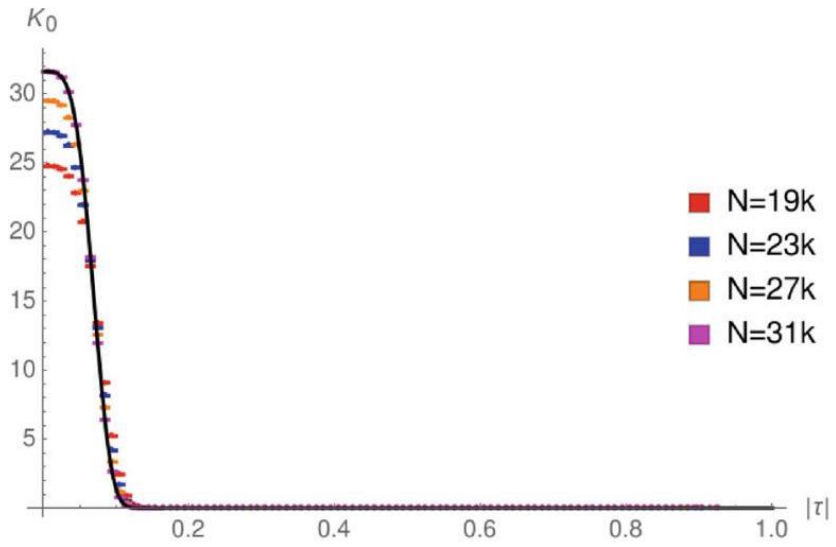

For the corresponding random variable, one can show that

对于对应的随机变量，可以证明

$$\lim_{\rho\to\infty}\left\langle K_m^{(4)}(x,x')\right\rangle = G_m^{(4)}(x,x')\,. \tag{22}$$

The hop-stop weights can be read off from Eq. (21) as $a=\frac{1}{2\pi}\sqrt{\frac{\rho}{6}}$ and $b=-\frac{m^2}{\rho}$, respectively.

跳停权重可分别从式 (21) 中读出，为 $a=\frac{1}{2\pi}\sqrt{\frac{\rho}{6}}$ 和 $b=-\frac{m^2}{\rho}$

$d=4$ dS and adS

$d=4$ dS 与反德西特空间

In $d=4$ for conformally flat spacetimes $g_{ab}=\Omega^2(x)\eta_{ab}$, the conformally coupled massless Green function is related to that in $\mathbb{M}^4$ by

在共形平直时空 $g_{ab}=\Omega^2(x)\eta_{ab}$ 的 $d=4$ 中，共形耦合无质量格林函数可通过下式与 $\mathbb{M}^4$ 中的格林函数联系起来

$$G_{0,\xi_c}(x,x')=\Omega^{-1}(x)\,G_0^F(x,x')\,\Omega^{-1}(x')\,, \tag{23}$$

where $\xi_c=\frac{1}{6}$ and $G_0^F(x,x')$ is the retarded massless Green function in $\mathbb{M}^4$. Further, if we have constant scalar curvature, the massive Green function for arbitrary ξ can be obtained from $G_{0,\xi_c}(x,x')$ using Eq. (8) because ξR is then a mass term.

其中 $\xi_c = \frac{1}{6}$ 和 $G_0^F(x,x')$ 是 $\mathbb{M}^4$ 中的 retarded 无质量格林函数。此外，若标量曲率为常数，任意 ξ 的有质量格林函数都可通过式 (8) 由 $G_{0,\xi_c}(x,x')$ 得到，因为此时 ξR 就是质量项。

In global dS spacetime and in the conformally flat patch of adS spacetime, it has been shown that [22]

研究表明，在整体德西特时空和反德西特时空的共形平直补丁中，有文献 [22] 指出

$$\lim_{\rho\to\infty} \frac{1}{2\pi}\sqrt{\frac{\rho}{6}}\,\langle L_0(x,x')\rangle = G_{0,\xi_c}(x,x')\,. \tag{24}$$

Therefore, we can construct the massive retarded Green function for arbitrary coupling from this along the same lines as before

因此，我们可以沿用之前的思路，由此构造任意耦合的有质量推迟格林函数

$$K^{(4)}_{m,\xi}(x,x') \equiv \sum_{k=0}^{\infty} a^k b^{k+1} L_k(x,x')\,. \tag{25}$$

with $a = \frac{1}{2\pi}\sqrt{\frac{\rho}{6}}$ and $b = -\frac{m^2+\left(\xi-\frac{1}{6}\right)R}{\rho}$.

其中包含 $a = \frac{1}{2\pi}\sqrt{\frac{\rho}{6}}$ 和 $b = -\frac{m^2+\left(\xi-\frac{1}{6}\right)R}{\rho}$ 。

Riemann Normal Neighborhoods

黎曼正规邻域

In more general spacetimes, it is a highly nontrivial task to find the average values of the random variable defined through the causal or link matrices. Due to this, it is not possible to prove if these random variables have the right continuum limit that we desire. However, there are still situations where we can make a more quantitative guess about the causal set Green function.

在更一般的时空中，求解通过因果矩阵或链路矩阵定义的随机变量的平均值是一项极为不平凡的任务。因此，我们无法证明这些随机变量是否能得到我们期望的正确连续极限。不过，仍有一些场景可以让我们对因果集格林函数做出更定量的推测。

For example, every $d = 2$ spacetime is locally conformally flat. If the spacetime is topologically trivial, then the MMC Green function equals the flat spacetime Green function Eq. (11). Therefore, it seems reasonable to expect, at least locally, that on causal sets sprinkled into such spacetimes, the massless minimally coupled causal set Green function, $K^{(2)}_{0,0}(x,x')$, is the flat one given by Eq. (13) and therefore for regions where R is approximately constant, that $K^{(2)}_{m,\xi}(x,x')$ is given by

例如，每个 $d=2$ 时空都是局部共形平坦的。如果该时空是拓扑平凡的，那么 MMC 格林函数就等于平直时空格林函数，即式 (11)。因此我们有理由认为，至少在局部，对于撒播到这类时空中的因果集，无质量最小耦合因果集格林函数 $K^{(2)}_{0,0}(x,x')$ 就是式 (13) 给出的平直时空格林函数，因此在 R 近似为常数的区域，$K^{(2)}_{m,\xi}(x,x')$ 由下式给出

$$K^{(2)}_{m,\xi}(x,x') = \sum_{k=0}^{\infty}\left(-\frac{m^2+\xi R}{\rho}\right)^k\left(\frac{1}{2}\right)^{k+1} C_k(x,x'), \tag{26}$$

The argument that the average value over sprinklings of the corresponding random variable will be the correct continuum Green function proceeds exactly as in the flat case. This is still a heuristic argument and cannot be made more concrete because $\langle C_k(x,x')\rangle$ is not known. The best we can do is show that the average value gives the right Green function in a Riemann normal neighborhood (RNN), in the continuum limit to leading order. Indeed, we find that when $m^2 \gg \xi R$

对应随机变量的撒播平均值就是正确的连续格林函数，这一论证过程和平直时空的情况完全一致。这仍只是一个启发式论证，由于 $\langle C_k(x,x')\rangle$ 尚未明确，无法得到更具体的结论。我们目前能做到的最佳结果是证明，在黎曼正规邻域 (RNN) 中，连续极限领头阶下，平均值给出正确的格林函数。实际上我们发现，当 $m^2 \gg \xi R$

$$\begin{aligned} G^{(2)}_{m,\xi}(x,x') &\approx \theta(x_0)\,\theta\left(\tau^2\right)\left[\frac{1}{2}J_0(m\tau) + \frac{R(x')\,\tau^2}{48}J_2(m\tau) - \frac{\xi R(x')\,\tau}{4m}J_1(m\tau)\right] \\ &= \lim_{\rho\to\infty}\left\langle K^{(2)}_{m,\xi}(x,x')\right\rangle \end{aligned} \tag{27}$$

One can prove a similar result in an RNN in $d=4$ starting with the link matrix with a further constraint that the average value matches only when $R_{ab}(x') \propto g_{ab}(x')$, i.e., for Einstein spaces. We refer the reader to [22] for more detail on these calculations.

我们可以在 $d=4$ 的黎曼正规邻域中得到类似结果，推导从带额外约束的链路矩阵出发，结果表明仅当 $R_{ab}(x') \propto g_{ab}(x')$ 时，也就是对爱因斯坦空间，平均值才匹配。更多相关计算细节读者可参考文献 [22]。

We emphasize that in the above constructions, the a priori knowledge of the continuum Green function was used to first propose an analogue on the causal set and then check if it gives the right continuum limit.

我们需要强调，上述构造过程中，我们利用了连续格林函数的先验知识，先在因果集上提出对应形式，再验证它能否给出正确的连续极限。

Before ending this section, we also mention two other, potentially more fundamental, proposals for constructing a Green function:

在本节结束前，我们还要介绍另外两种可能更基本的格林函数构造方案:

- using d'Alembertians: In the continuum, we expect there is an inverse relation between the d'Alembertian and the Green function (with appropriate boundary conditions). It is reasonable to expect that such a relation might exist for the analogous objects in the causal set. As mentioned in the introduction, there

are well-studied proposals for constructing d'Alembertians on causal sets. These d'Alembertians are, by construction, retarded i.e., they are built out of layers in the past of a given causal set element, one might expect that their inverse (In the causal set, this is a simple matrix inversion.) should therefore define some sort of retarded Green function. The important question is whether this is the retarded Green function we want, i.e., the one that gives the right continuum limit. Such a "sweety-salty" duality has been shown in a limited context [18] of $\mathbb{M}^4$ but might be more general.

- 利用达朗贝尔算符: 在连续理论中，我们认为达朗贝尔算符和格林函数 (在合适的边界条件下) 存在互逆关系。我们有理由推测这种关系也存在于因果集的对应对象之间。正如引言中提到的，已有大量研究提出了在因果集上构造达朗贝尔算符的方案。根据构造，这些达朗贝尔算符都是推迟的，即它们由给定因果集元素过去的分层构建而来，因此我们可以预期它们的逆 (在因果集中这是简单的矩阵求逆) 可以定义某种推迟格林函数。核心问题在于，这是否就是我们需要的推迟格林函数，即能否给出正确的连续极限。这种"甜-咸"对偶已经在 $\mathbb{M}^4$ 的有限场景下被证明 [18]，但它可能具有更广泛的适用性。

- using preferred past: A more recent proposal for constructing a Green function augments the causal set (Another such attempt was made earlier on by introducing a slicing and using it to define discrete d'Alembertians [15].) with a preferred past structure in order to first define a d'Alembertian and then a retarted Green function. This is motived from ideas in local algebraic quantum field theory [9]. The preferred past structure is a map Λ such that the preferred past $\Lambda(p)$ of a point p is a point of rank (Rank in this context means the minimum number of links in a path between two points.) 2 in the past of p . In general, this structure can be chosen in different ways, and it is not clear which is the most appropriate choice. An example of theory construction for a regular diamond lattice using this method is shown in [9].

- 利用优先过去: 这是一个更新的格林函数构造方案，它给因果集引入了优先过去结构，以便先定义达朗贝尔算符，再得到推迟格林函数 (此前也有过类似尝试，通过引入切片构造离散达朗贝尔算符 [15])。该方案的动机来自局域代数量子场论的思想 [9]。优先过去结构是一个映射 Λ ，满足点 p 的优先过去 $\Lambda(p)$ 是 p 过去中秩为 2 的点 (该语境下秩指两点之间路径的最少链路数)。一般来说，这种结构可以有多种不同的选择，目前尚不清楚哪一种是最合适的。文献 [9] 给出了用该方法构造规则金刚石晶格理论的例子。

SJ in the Continuum

连续统中的 SJ 构造

The next step in the construction is the choice of a state. Consider a region with finite volume V in (M, g) . For a free scalar field in this region, the Klein-Gordon (KG) equation is

该构造的下一步是选择一个量子态。考虑 (M, g) 中体积有限的区域 V 。对于该区域内的自由标量场，克莱因-戈登 (KG) 方程为

$$\left(\widehat{\Box} - m^2\right)\phi = 0, \tag{28}$$

where $\widehat{\square} \equiv g^{ab}\nabla_a\nabla_b$, and the effective mass $m^2 = m_p^2 + \xi R$, where m_p is the physical mass, R is the scalar curvature and ξ is the coupling. Let $\{u_{\mathbf{q}}\}$ be a complete set of modes satisfying the KG equation in (M, g) and orthonormal with respect to the KG inner product

其中 $\widehat{\square} \equiv g^{ab}\nabla_a\nabla_b$ ，有效质量 $m^2 = m_p^2 + \xi R$ 满足关系，m_p 为物理质量，R 为标量曲率，ξ 为耦合常数。设 $\{u_{\mathbf{q}}\}$ 是满足 (M, g) 内 KG 方程、且关于 KG 内积标准正交的完备模集合

$$(f, g)_{\mathrm{KG}} = \int_{\sum} (f^* \nabla_a g - g^* \nabla_a f)\, dS^a, \tag{29}$$

where $\sum$ is a Cauchy hypersurface in (M, g) . The field operator corresponding to the classical field can be expressed as a mode expansion with respect to this set:

其中 $\sum$ 是 (M, g) 中的柯西超曲面。对应经典场的场算符可以对该集合做模展开:

$$\widehat{\Phi}(x) \equiv \sum_{\mathbf{q}} \hat{\mathbf{a}}_{\mathbf{q}} u_{\mathbf{q}}(x) + \hat{\mathbf{a}}_{\mathbf{q}}^{\dagger} u_{\mathbf{q}}^*(x), \tag{30}$$

with $\hat{\mathbf{a}}_{\mathbf{q}}, \hat{\mathbf{a}}_{\mathbf{q}}^{\dagger}$ satisfying the commutation relations

其中 $\hat{\mathbf{a}}_{\mathbf{q}}, \hat{\mathbf{a}}_{\mathbf{q}}^{\dagger}$ 满足对易关系

$$\left[\hat{\mathbf{a}}_{\mathbf{q}}, \hat{\mathbf{a}}_{\mathbf{q}'}^{\dagger}\right] = \delta_{\mathbf{q}\mathbf{q}'}, \ \left[\hat{\mathbf{a}}_{\mathbf{q}}, \hat{\mathbf{a}}_{\mathbf{q}'}\right] = 0, \ \left[\hat{\mathbf{a}}_{\mathbf{q}}^{\dagger}, \hat{\mathbf{a}}_{\mathbf{q}'}^{\dagger}\right] = 0. \tag{31}$$

The covariant commutation relations for the scalar field operator are given by the Peierls bracket:

标量场算符的协变对易关系由佩尔斯括号给出:

$$\left[\widehat{\Phi}(x), \widehat{\Phi}(x')\right] = i\Delta(x, x'), \tag{32}$$

where the Pauli-Jordan (PJ) function $\Delta(x, x')$ is given by

其中泡利-约旦 (PJ) 函数 $\Delta(x, x')$ 由下式给出

$$\Delta(x, x') \equiv G_R(x, x') - G_A(x, x'), \tag{33}$$

with $G_{R,A}(x, x')$ being the retarded and advanced Green functions, respectively. This can also be written in terms of the modes $\{u_{\mathbf{q}}\}$ using the mode expansion and the commutation relations:

其中 $G_{R,A}(x, x')$ 分别是推迟格林函数和超前格林函数。利用模展开和对易关系，它也可以用模 $\{u_{\mathbf{q}}\}$ 写为:

$$i\Delta(x, x') = \sum_{\mathbf{q}} u_{\mathbf{q}}(x)\, u_{\mathbf{q}}^*(x') - u_{\mathbf{q}}^*(x)\, u_{\mathbf{q}}(x'), \tag{34}$$

and the two-point function or the state/vacuum (In the usual language of Fock spaces, the vacuum would be $\hat{\mathbf{a}}_{\mathbf{q}}|0\rangle = 0$.) associated with these modes is defined as the positive part of the above expansion:

与这些模关联的两点函数，即态/真空 (在福克空间的常规语言中，真空为 $\hat{\mathbf{a}}_{\mathbf{q}}|0\rangle = 0$)，定义为上述展开的正部分:

$$W(x,x') \equiv \sum_{\mathbf{q}} u_{\mathbf{q}}(x)\, u^{*}_{\mathbf{q}}(x')\,. \tag{35}$$

The initial choice of modes is usually motivated by a choice of observer or the symmetries of the background spacetime. The SJ state or equivalently the SJ modes are constructed directly from $i\widehat{\Delta}$ in any given finite spacetime region, do not require a choice of observer, and are thus unique. The question of physical interpretation of the SJ state is more nuanced and has been studied in some special cases [1].

初始的模选择通常由观测者选择或背景时空的对称性驱动。SJ 态 (等价于 SJ 模) 可在任意给定有限时空区域中直接由 $i\widehat{\Delta}$ 构造，不需要选择观测者，因此是唯一的。SJ 态的物理解释更为微妙，目前已在一些特殊情形中得到研究 [1]。

To construct the SJ vacuum from the PJ function, it is elevated to an integral operator as follows:

为了从 PJ 函数构造 SJ 真空，我们将其提升为如下积分算符:

$$i\widehat{\Delta} \circ f \equiv i\int_{V} \Delta(x,x')\, f(x')\, dV_{x'} \tag{36}$$

which acts on $\mathcal{L}^2$ functions in V and where

该算符作用在 V 内的 $\mathcal{L}^2$ 函数上，其中

$$\langle f, g \mid f, g\rangle = \int_{V} dV_x f^{*}(x)\, g(x) \tag{37}$$

is the $\mathcal{L}^2$ inner product. Since $\Delta(x,x')$ is antisymmetric in its arguments, $i\widehat{\Delta}$ is Hermitian on the space of $\mathcal{L}^2$ functions in V . Its nonzero eigenvalues, given by

是 $\mathcal{L}^2$ 内积。由于 $\Delta(x,x')$ 关于其自变量反对称，$i\widehat{\Delta}$ 在 V 内的 $\mathcal{L}^2$ 函数空间上是厄米算符。它的非零特征值由下式给出

$$i\widehat{\Delta} \circ \tilde{s}_{\mathbf{k}}(x) = \int_{V} dV_{x'}\, i\Delta(x,x')\, \tilde{s}_{\mathbf{k}}(x') = \lambda_{\mathbf{k}} \tilde{s}_{\mathbf{k}}(x) \tag{38}$$

therefore come in pairs $(\lambda_{\mathbf{k}}, -\lambda_{\mathbf{k}})$, corresponding to the eigenfunctions $\left(\tilde{s}^{+}_{\mathbf{k}}, \tilde{s}^{-}_{\mathbf{k}}\right)$ where $\tilde{s}^{-}_{\mathbf{k}} = \left(\tilde{s}^{+}_{\mathbf{k}}\right)^{*}$ (We adopt the notation that the $\tilde{s}_k$ are the un-normalized (with respect to the $\mathcal{L}^2$ norm) SJ eigenfunctions, whereas the s_k without the tilde are the normalized SJ eigenfunctions.). One therefore has an intrinsic and coordinate-/observer-independent separation of positive and negative eigenmodes of $i\widehat{\Delta}$.

因此特征值成对出现 $(\lambda_{\mathbf{k}}, -\lambda_{\mathbf{k}})$，对应本征函数 $\left(\tilde{s}^{+}_{\mathbf{k}}, \tilde{s}^{-}_{\mathbf{k}}\right)$，其中 $\tilde{s}^{-}_{\mathbf{k}} = \left(\tilde{s}^{+}_{\mathbf{k}}\right)^{*}$ (我们采用如下记号: $\tilde{s}_k$ 是未归一化 (关于 $\mathcal{L}^2$ 范数) 的 SJ 本征函数，而不带波浪号的 s_k 是归一化的 SJ 本征函数)。因此我们可以得到 $i\widehat{\Delta}$ 正负本征模之间，不依赖坐标与观测者的内禀区分。

The central idea of the construction is the following observation [26,30]:

该构造的核心思想来自如下观察 [26,30]:

$$\mathrm{Ker}\left(\widehat{\Box} - m_p^2\right) = \overline{\mathrm{Im}\left(\widehat{\Delta}\right)}, \tag{39}$$

where the operators are defined in V (In a spacetime of constant scalar curvature, m defined above is constant, and hence this result continues to hold when m_p is replaced by m .). This means that the eigenvectors in the image of $i\widehat{\Delta}$ (i.e., excluding those in $\mathrm{Ker}\left(i\widehat{\Delta}\right)$) span the full solution space of the KG operator. Along with our earlier result that these eigenvectors have a separation into those with positive eigenvalues and those with negative eigenvalues, we get a unique decomposition of the field operator:

其中算符定义在 V 中 (在常标量曲率时空中，上述定义的 m 是常数，因此当 m_p 替换为 m 时，该结果仍然成立)。这意味着 $i\widehat{\Delta}$ 像中的本征向量 (即排除 $\mathrm{Ker}\left(i\widehat{\Delta}\right)$ 中的本征向量) 张成了 KG 算符的全解空间。结合我们此前得到的结论——这些本征向量可分为正本征值和负本征值两类，我们得到场算符的唯一分解:

$$\widehat{\Phi}(x) = \sum_{\mathbf{k}} \hat{\mathbf{b}}_{\mathbf{k}} s_{\mathbf{k}}(x) + \hat{\mathbf{b}}^{\dagger}_{\mathbf{k}} s^{*}_{\mathbf{k}}(x), \tag{40}$$

and the SJ vacuum state is defined as

因此 SJ 真空态定义为

$$\hat{\mathbf{b}}_{\mathbf{k}} |0_{SJ}\rangle = 0 \ \forall \mathbf{k}, \tag{41}$$

where

其中

$$s_{\mathbf{k}} = \sqrt{\lambda_{\mathbf{k}}}\tilde{s}^{+}_{\mathbf{k}} \tag{42}$$

are the normalized *SJ* modes which form an orthonormal set in $\overline{\mathrm{Im}\left(i\widehat{\Delta}\right)}$ with respect to the $\mathcal{L}^2$ norm

是归一化的 *SJ* 模，它们在 $\overline{\mathrm{Im}\left(i\widehat{\Delta}\right)}$ 中关于 $\mathcal{L}^2$ 范数构成一组标准正交基

$$\langle s_{\mathbf{k}}, s_{\mathbf{k}'} \mid s_{\mathbf{k}}, s_{\mathbf{k}'}\rangle = \lambda_{\mathbf{k}}\delta_{\mathbf{k}\mathbf{k}'}$$

$$\left\langle s^{*}_{\mathbf{k}}, s_{\mathbf{k}'} \mid s^{*}_{\mathbf{k}}, s_{\mathbf{k}'}\right\rangle = 0 \tag{43}$$

Using the spectral decomposition

利用谱分解

$$i\Delta(x,x') = \sum_{\mathbf{k}} s_{\mathbf{k}}(x)\, s^*_{\mathbf{k}}(x') - s^*_{\mathbf{k}}(x)\, s_{\mathbf{k}}(x'), \tag{44}$$

the SJ two-point function in V is the positive part of $i\widehat{\Delta}$:

V 中的 SJ 两点关联函数是 $i\widehat{\Delta}$ 的正部:

$$W_{\mathrm{SJ}}(x,x') \equiv \sum_{\mathbf{k}} s_{\mathbf{k}}(x)\, s^*_{\mathbf{k}}(x'). \tag{45}$$

If $W_{\mathrm{SJ}}(x,x')$ remains well-defined as the IR cutoff (i.e., V) is taken to infinity, this defines the SJ vacuum in the full spacetime (M,g) .

若当红外截断 (即 V) 取至无穷时 $W_{\mathrm{SJ}}(x,x')$ 仍保持良定义，这就定义了全时空 (M,g) 中的 SJ 真空。

Alternately, the SJ two-point function is uniquely defined most generally by the following conditions [26]:

另外，在最一般的情况下 SJ 两点关联函数可由以下条件唯一确定 [26]:

$$i\Delta(x,x') = W_{\mathrm{SJ}}(x,x') - W_{\mathrm{SJ}}(x',x),$$

$$\int_V dV' \int_V dV f^*(x')\, W_{\mathrm{SJ}}(x',x)\, f(x) \geq 0, \quad \text{(Positive Semidefinite)}$$

$$\int_V dV' W_{\mathrm{SJ}}(x,x')\, W^*_{\mathrm{SJ}}(x',x'') = 0, \quad \text{(Ground state or Purity)} \tag{46}$$

The first condition follows from the definition of the Wightman function. The motivation for the second condition can be seen as follows - given a state vector $|0\rangle$ in some Hilbert space, the above result can be derived as a theorem | that follows immediately from the positivity of $\| \psi\|^2 = \langle \psi \mid \psi \rangle$ where $|\psi\rangle = \int dV(x) f(x) \widehat{\phi} |0\rangle$. The utility of the final conditio mention that this condition helps in picking out, from a set of solutions, those that match the notion of a ground state when such a notion is available. For example, it has been shown that the SJ vacuum will coincide with the minimum energy vacuum in stationary spacetimes [1, 2] . In other cases this condition implies that the entanglement entropy associated with W_{SJ} vanishes, i.e., the SJ state is always pure. We refer the reader to [26] for a simple example of these conditions in action.

第一个条件由威曼函数的定义直接得到。第二个条件的动机可以解释如下: 给定态矢量 $|0\rangle$ in some Hilbert space, the above result can be derived as a theorem | , 它直接来自 $\| \psi\|^2 = \langle \psi \mid \psi \rangle$ 的正定性, 其中 $|\psi\rangle = \int dV(x) f(x) \widehat{\phi} |0\rangle$. The utility of the final condition is not as obvious; we just | 指出，当基态这一概念存在时，该条件可以帮助我们从一组解中选出符合基态概念的解。例如，已有研究证明，在定态时空 [1, 2] 中 SJ 真空与最小能量真空一致。在其他情况下该条件意味着与 W_{SJ} 关联的纠缠熵为零，即 SJ 态始终是纯态。关于这些条件的简单应用实例，读者可参见文献 [26]。

A third way to obtain the SJ modes is via a mode comparison using Bogoliubov coefficients [1]. Given the equality in Eq. (39) between $\overline{\mathrm{Im}\left(\widehat{\Delta}\right)}$ and the KG solution space, there must exist a transformation between the KG modes $\{u_{\mathbf{q}}\}$ in V and the SJ modes $\{s_{\mathbf{k}}\}$, even if the former are not orthonormal with respect to the $\mathcal{L}^2$ inner product. Namely, we can write:

得到 SJ 模的第三种方法是利用 Bogoliubov 系数做模比较 [1]。由于式 (39) 中 $\overline{\mathrm{Im}\left(\widehat{\Delta}\right)}$ 与 KG 解空间相等，因此即使 KG 模关于 $\mathcal{L}^2$ 内积不是正交的，V 中的 KG 模 $\{u_{\mathbf{q}}\}$ 和 SJ 模 $\{s_{\mathbf{k}}\}$ 之间也一定存在变换，即我们可以写出:

$$s_{\mathbf{k}}(x) = \sum_{\mathbf{q}} u_{\mathbf{q}}(x) A_{\mathbf{qk}} + u^*_{\mathbf{q}}(x) B_{\mathbf{qk}}, \tag{47}$$

where $A_{\mathbf{qk}} = \left(u_{\mathbf{q}}, s_{\mathbf{k}}\right)_{\mathrm{KG}}, B_{\mathbf{qk}} = \left(u^*_{\mathbf{q}}, s_{\mathbf{k}}\right)_{\mathrm{KG}}$ and they satisfy the constraints:

其中 $A_{\mathbf{qk}} = \left(u_{\mathbf{q}}, s_{\mathbf{k}}\right)_{\mathrm{KG}}, B_{\mathbf{qk}} = \left(u^*_{\mathbf{q}}, s_{\mathbf{k}}\right)_{\mathrm{KG}}$，它们满足约束:

$$\begin{aligned}
\sum_{\mathbf{q}} \mathbf{A}_{\mathbf{qk}'} A^*_{\mathbf{qk}} - \mathbf{B}_{\mathbf{qk}'} B^*_{\mathbf{qk}} &= \delta_{\mathbf{kk}'} \\
\sum_{\mathbf{q}} \mathbf{B}_{\mathbf{qk}'} A_{\mathbf{qk}} - \mathbf{A}_{\mathbf{qk}'} B_{\mathbf{qk}} &= 0.
\end{aligned} \tag{48}$$

Further, if the KG modes themselves satisfy the $\mathcal{L}^2$ orthonormality condition

此外，如果 KG 模自身满足 $\mathcal{L}^2$ 正交归一条件

$$\left\langle u_{\mathbf{q}}, u_{\mathbf{q}'} \right\rangle = \delta_{qq'}, \ \left\langle u^*_{\mathbf{q}}, u_{\mathbf{q}'} \right\rangle = 0, \tag{49}$$

the constraints simplify considerably.

约束会大幅简化。

It is important to note that the above calculations are limited to finite V. There are subtleties in identifying $\mathrm{Ker}\left(\widehat{\Box} - m^2\right)$ in V, starting from the solutions in full spacetime.

需要注意的是，上述计算仅局限于有限 V。从全时空的解出发，在 V 中确定 $\mathrm{Ker}\left(\widehat{\Box} - m^2\right)$ 存在一些微妙的问题。

An important question is whether the limits involved in these approaches commute. In the first two approaches, we define the SJ vacuum directly in finite V and only take the limit $V \to \infty$ at the end, if possible, whereas in the mode comparison approach, we might have to take the limit for the comparison. A case in point is the 2d causal diamond in Minkowski spacetime, where, in order to compare with the IR limit, $W(x, x')$ was studied in a small region in the interior of the larger diamond, which to leading order was found to have the form of the (IR-regulated) 2d Minkowski vacuum [2]. Similar considerations come up in [1,3] when using the Bogoliubov method.

一个重要问题是这些方法中涉及的极限是否可交换。在前两种方法中，我们直接在有限 V 下定义了 SJ 真空，仅在可行的情况下最后才取极限 $V \to \infty$；而在模比较方法中，我们可能必须为比较过程提前取极限。一个典型例子就是闵氏时空下的二维因果菱形: 为了和红外极限比较，研究者在大菱形内部的一个小区域中研究了 $W(x, x')$，发现在领头阶下它具有 (红外正规化的) 二维闵氏真空的形式 [2]。文献 [1,3] 在使用博戈留波夫方法时也遇到了类似的问题。

Before moving on to the construction in the causal set, we mention the Hadamard condition, which is related to the UV behavior of two-point functions. It has been shown [8, 13] that the SJ state in the continuum is not Hadamard. Further, one can obtain a Hadamard state by introducing a smoothening function in the definition of the PJ operator; this has been tested in static and cosmological spacetimes [8]. However, the introduction of such a smoothening function introduces nonuniqueness into the construction. Whether a unique, physically motivated choice can be made for such a function remains an open question. While working with causal sets, the Hadamard condition becomes a nonissue since there is natural discreteness and the question of UV limiting behavior does not arise.

在进入因果集的构造之前，我们来介绍一下哈达玛条件，该条件与两点函数的紫外行为相关。已有证明 [8, 13]，连续统中的 SJ 态不是哈达玛态。此外，可以通过在 PJ 算子的定义中引入平滑函数来得到哈达玛态；这已经在静态时空和宇宙学时空中得到了验证 [8]。但引入这类平滑函数会给构造过程带来非唯一性。能否找到一个满足物理要求的唯一选择，目前仍是一个开放问题。在因果集中工作时，哈达玛条件不再是问题，因为因果集本身具有自然离散性，不会产生紫外极限行为的问题。

SJ in the Causal Set

因果集中的 SJ

Causal sets are a natural covariant discretisation of the continuum; they also contain important signatures of quantum spacetime. This makes the results of simulations on causal sets interesting. As mentioned before, the SJ construction simplifies drastically when working with causal sets because the central eigenvalue equation for the PJ operator is now reduced to a matrix equation. Therefore, simulations are only limited by the size of the matrices involved, which is the same as the size of the causal set.

因果集是连续统自然满足协变性的离散化形式，还包含量子时空的重要特征。这使得因果集上的模拟结果十分有研究价值。如前文所述，在处理因果集时 SJ 构造会大幅简化，因为 PJ 算符的核心本征方程现在被约化为矩阵方程。因此，模拟仅受限于相关矩阵的大小，而矩阵大小和因果集的规模一致。

Before we present examples, a quick dimensional analysis tells us the right quantities to compare - the retarded Green function in the continuum satisfies the KG equation so ([] refers to length dimension.) $[G] = 2 - d = [\Delta] = [W]$. Therefore, $[\lambda_k] = 2$ and the normalized eigenfunctions have $[s_{\mathbf{k}}] = 1 - d/2$.

在我们给出例子之前，快速量纲分析就能告诉我们需要比较的合适物理量——连续统中的推迟格林函数满足克莱因-戈登方程，因此 ([] 指长度量纲) $[G] = 2 - d = [\Delta] = [W]$。因此，$[\lambda_k] = 2$，归一化本征函数具有 $[s_{\mathbf{k}}] = 1 - d/2$。

In the causal set, we get the dimension of the massless Green function K_0 by requiring that $\left[K_0 m^2/\rho\right] = 0$, where $\left[m^2/\rho\right] = d-2$. This gives $[K_0] = 2-d = [G] = [i\Delta]$. Using the correspondence $\int dV_y \to \frac{1}{\rho}\sum_y$, the eigenvalue equation becomes a matrix equation:

在因果集中，我们通过要求 $\left[K_0 m^2/\rho\right] = 0$ 得到无质量格林函数的量纲 K_0 ，其中 $\left[m^2/\rho\right] = d-2$ 。由此可得 $[K_0] = 2-d = [G] = [i\Delta]$ 。利用对应关系 $\int dV_y \to \frac{1}{\rho}\sum_y$ ，本征方程变为矩阵形式:

$$\frac{1}{\rho} i\Delta f_k = \lambda_k f_k \tag{50}$$

where (In simulations the $1/\rho$ factor in Eq. (50) is omitted, which is why in the figures showing the eigenvalues are divided by ρ .) $[\lambda_k] = 2$.

其中 (模拟中省略了式 (50) 中的 $1/\rho$ 因子，这就是为什么图中显示的本征值都除以了 ρ 。) $[\lambda_k] = 2$ 。

As in the continuum, we have (Here, normalization is obtained by taking the dot product of the vector with itself, divided by the density.) $[s_{\mathbf{k}}] = 1 - d/2$. Further, $[W] = 2-d$ and can be compared directly with its counterpart in the continuum.

和在连续统中一样，我们有 (此处归一化通过将向量自身点积除以密度得到) $[s_{\mathbf{k}}] = 1 - d/2$ 。此外，$[W] = 2-d$ ，可以直接和它在连续统中的对应量比较。

We show numerical results for the causal set SJ vacuum for four cases $[2,28]-$ causal diamonds in 2 d and 4 d Minkowski spacetime and slabs of 2 d and 4 d global de Sitter spacetime. In all cases we show how the spectrum of the PJ operator compares between the continuum and the causal set. We also show the SJ vacuum and its comparison with the continuum, whenever applicable. Note that, where visible, error bars in the binned data reflect the standard error of the mean (SEM).

我们给出四种情况下因果集 SJ 真空的数值结果 $[2,28]-$: 2 d 维和 4 d 维闵氏时空的因果菱形，以及 2 d 维和 4 d 维全局德西特时空的 slab 区域。在所有情况中，我们都展示了连续统和因果集的 PJ 算符谱的对比。我们还在适用的情况下给出了 SJ 真空及其与连续统结果的对比。请注意，在可观测处，分仓数据的误差棒反映的是均值标准误差 (SEM)。

Causal Diamond in $\mathbb{M}^2$

$\mathbb{M}^2$ 中的因果菱形

The IR-regulated Minkowski two-point function is

红外调节后的闵氏两点关联函数为

$$\mathrm{Re}\left[W_{\mathrm{mink}}\right] = -\frac{1}{2\pi}\ln(x) + c_1,\ x = \tau \text{ or } d, \tag{51}$$

where τ, d are the timelike, spacelike distances, respectively and c_1 depends on the IR cutoff. In [2] it was shown that in a small subregion in the center of the causal diamond (i.e., away from the boundaries)

其中 τ, d 分别为类时距离和类空距离，c_1 依赖于红外截断。文献 [2] 已证明，在因果菱形中心的小子区域内 (即远离边界处)

$$c_1 \approx -\frac{1}{2\pi}\ln\left(\lambda e^{\gamma}\right), \tag{52}$$

where γ is the Euler-Mascheroni constant and $\lambda \sim 0.46/L$, and where $2L$ is the side length of the diamond. In units where the volume (area in $2d$) of the diamond is unity, $L = 1/2$ and $c_1 \approx -0.0786$.

其中 γ 为欧拉-马歇罗尼常数，$\lambda \sim 0.46/L$ ，且 $2L$ 为菱形的边长。在菱形体积 ($2d$ 中为面积) 为 1 的单位制下，$L = 1/2$ 且 $c_1 \approx -0.0786$ 。

Simulation results are shown in Figs. 2, 3, and 4. Figure 2 is a log-log plot of the positive causal set SJ eigenvalues, along with the positive continuum eigenvalues - the two sets of eigenvalues are in agreement up to a characteristic "knee" at which the causal set spectrum dips and ceases to obey a power-law with exponent -1 . Specifically, the causal set SJ eigenvalues can be modeled as $\lambda^{\mathrm{CS}} = \beta_1/n^{\alpha} + \beta_2 n + \beta_3$. Importantly, there is a smooth, linear regime in the UV, and this nonscaling behavior could indicate new physics. There is also a clear convergence of the spectrum with causal set size N except that the knee is pushed to smaller eigenvalues as N increases. We see these patterns in all cases that we consider.

模拟结果展示在图 2、图 3 和图 4 中。图 2 是正因果集 SJ 本征值的双对数图，同时给出了连续谱正本征值——两组本征值在特征"拐点"前一致，在拐点处因果集谱下降，不再服从指数为-1 的幂律。具体而言，因果集 SJ 本征值可建模为 $\lambda^{\mathrm{CS}} = \beta_1/n^{\alpha} + \beta_2 n + \beta_3$ 。重要的是，紫外区存在光滑的线性区域，这种非标度行为可能预示新物理。谱也随因果集尺寸 N 明显收敛，仅当 N 增大时，拐点向更小的本征值移动。我们在所有研究案例中都观测到了这一规律。

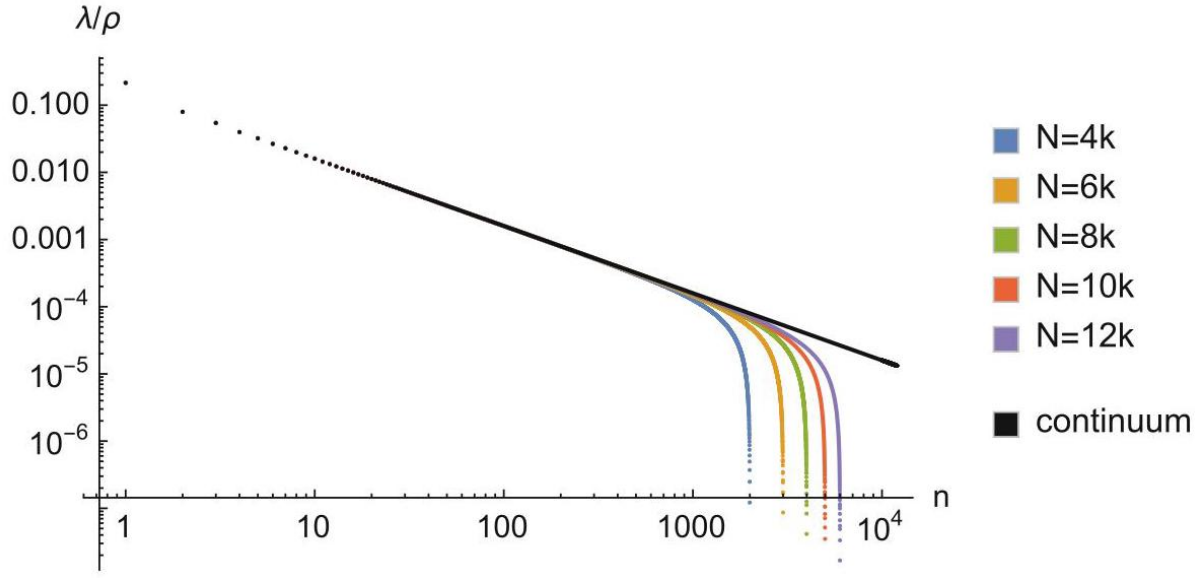

Fig. 2 Log-log plot of the eigenvalues of $i\Delta$ divided by density ρ (for the causal sets, the continuum spectrum is the straight black line), in the 2 d causal diamond; $m = 0$

图 2 2 d 因果菱形中，$i\Delta$ 本征值除以密度 ρ 的双对数图 (因果集结果，连续谱为黑色直线)；$m = 0$

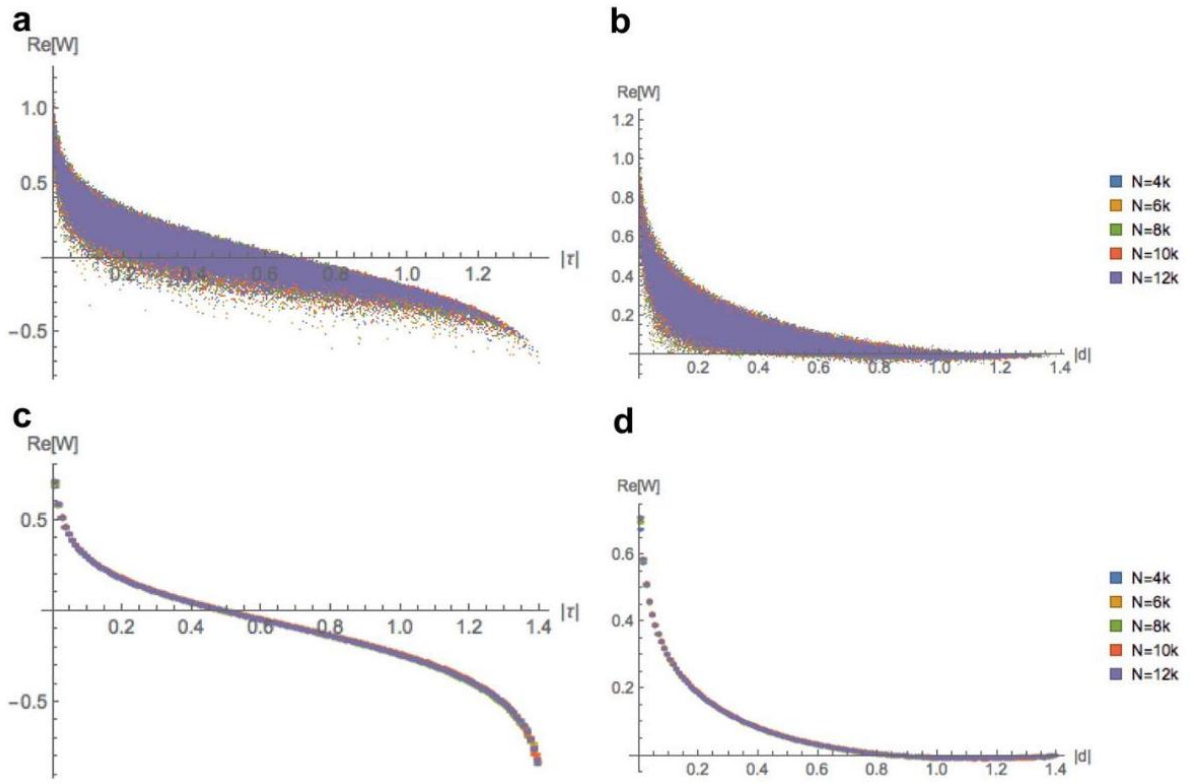

Fig. 3 (a)-(b) represent $\mathrm{Re}\,[W_{\mathrm{SJ}}]$ vs. geodesic distance for a sample of 100000 randomly selected pairs, in the 2d causal diamond; $m = 0$. (c)-(d) are plots of the binned and averaged data with the SEM. (a) Causal. (b) Spacelike. (c) Causal. (d) Spacelike

图 3 (a)-(b) 为二维因果菱形中，100000 对随机选取事件对的 $\mathrm{Re}\,[W_{\mathrm{SJ}}]$ 随测地线距离的变化；$m = 0$ 。(c)-(d) 是分 bin 平均后带标准误的图。(a) 类时；(b) 类空；(c) 类时；(d) 类空

Figure 3 shows scatter plots of $\mathrm{Re}\,[W_{\mathrm{SJ}}]$ for pairs of events that are causally and spacelike related; it also shows the binned and averaged plots where the convergence becomes clear. The convergence with N is very good and tells us that we are in the asymptotic regime, i.e., N is large enough. A comparison with the continuum is shown in Fig. 4; it shows the scatter plots and the binned and averaged plots for W_{SJ} within a smaller diamond of side length 1/4 compared to that of the original diamond it is concentric to. The continuum IR-regulated Minkowski curve is also plotted. These plots confirm that away from the boundaries of the diamond $\mathrm{Re}\,[W_{\mathrm{SJ}}]$ indeed resembles the Minkowski vacuum.

图 3 展示了类时关联和类空关联事件对的 $\mathrm{Re}\,[W_{\mathrm{SJ}}]$ 散点图，同时给出了分 bin 平均后的图，收敛性在其中清晰可见。随 N 的收敛性非常好，说明我们处于渐近区域，即 N 足够大。与连续谱的对比展示在图 4 中，图 4 给出了原大菱形同心小子菱形 (边长为 1/4) 内 W_{SJ} 的散点图和分 bin 平均图。同时也绘制了红外调节后的连续闵氏曲线。这些图证实，在远离菱形边界的区域，$\mathrm{Re}\,[W_{\mathrm{SJ}}]$ 确实与闵氏真空一致。

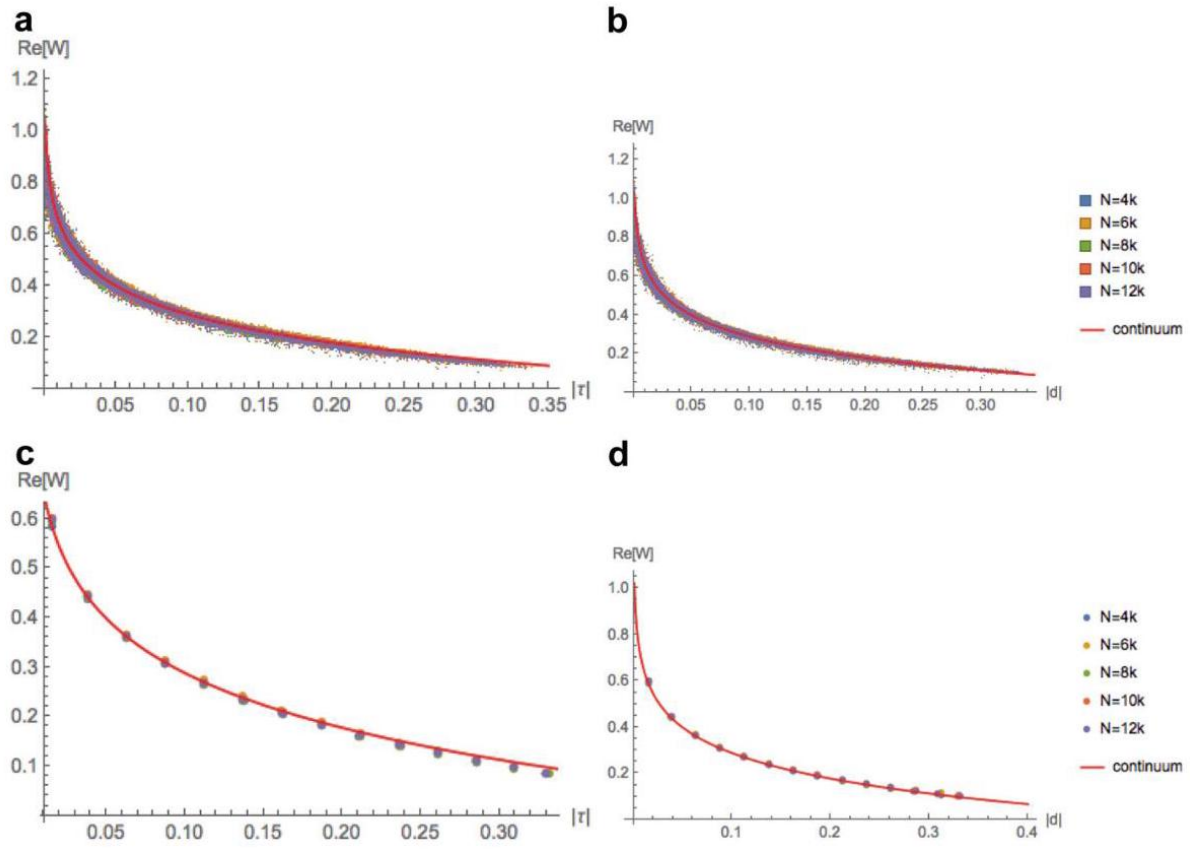

Fig. 4 (a)-(b) represent $\mathrm{Re}\,[W_{\mathrm{SJ}}]$ vs. geodesic distance for all pairs within a sub-diamond with side length 1/4 of that the full diamond, in the 2 d causal diamond; $m = 0$. (c)-(d) are plots of the binned and averaged data with the SEM. In both cases, the continuum IR-regulated Minkowski Wightman function Eq. (51) is also shown. (a) Causal. (b) Spacelike. (c) Causal. (d) Spacelike

图 4 (a)-(b) 为 2 d 因果菱形中，边长为原全菱形边长 1/4 的子菱形内所有事件对的 $\mathrm{Re}\,[W_{\mathrm{SJ}}]$ 随测地线距离的变化；$m = 0$ 。(c)-(d) 是分 bin 平均后带标准误的图。两种情况均同时给出了连续红外调节闵氏维特曼函数式 (51)。(a) 类时；(b) 类空；(c) 类时；(d) 类空

Causal Diamond in $\mathbb{M}^4$

$\mathbb{M}^4$ 中的因果菱形

The 4d Minkowski two-point function is

四维闵氏两点关联函数为

$$\mathrm{Re}\,[W_{\mathrm{mink}}] = \frac{1}{4\pi^2 x^2},\ x = i\tau \text{ or } |d|\,, \tag{53}$$

and we work in units where the height of the diamond is unity.

我们采用自然单位制，令菱形的高度为 1

In Fig. 5 we show the log-log plot of the SJ spectrum which converges well as N is increased, except near the knee which, as in the 2d diamond, shifts to the UV as N increases. Also, there is no analytic calculation of the SJ spectrum in this case to compare with.

图 5 给出了 SJ 能谱的双对数图，当 N 增大时，除拐点附近外能谱收敛性良好；和二维菱形的情况一样，随着 N 增加，拐点向紫外方向移动。此外，该情况暂无 SJ 能谱的解析计算结果可用于对比。

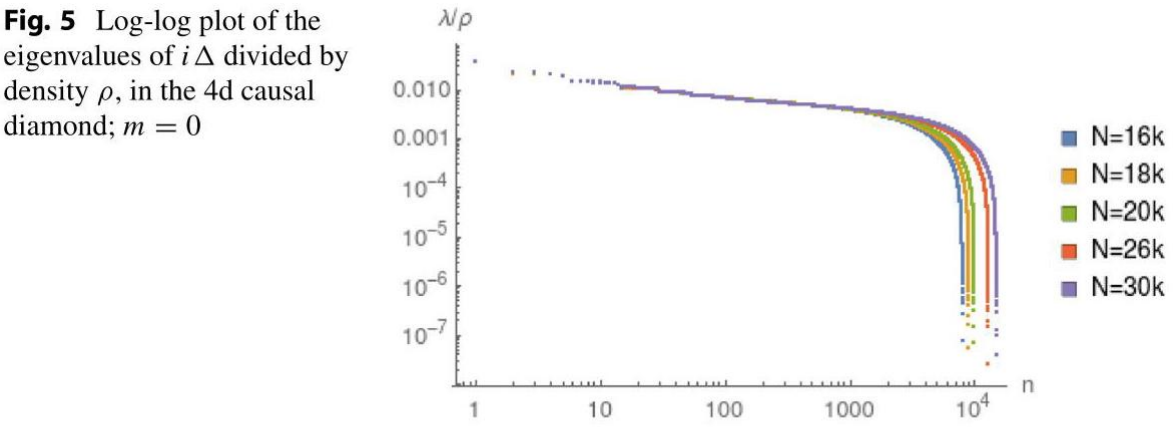

Fig. 5 Log-log plot of the eigenvalues of $i\Delta$ divided by density ρ, in the 4d causal diamond; $m = 0$

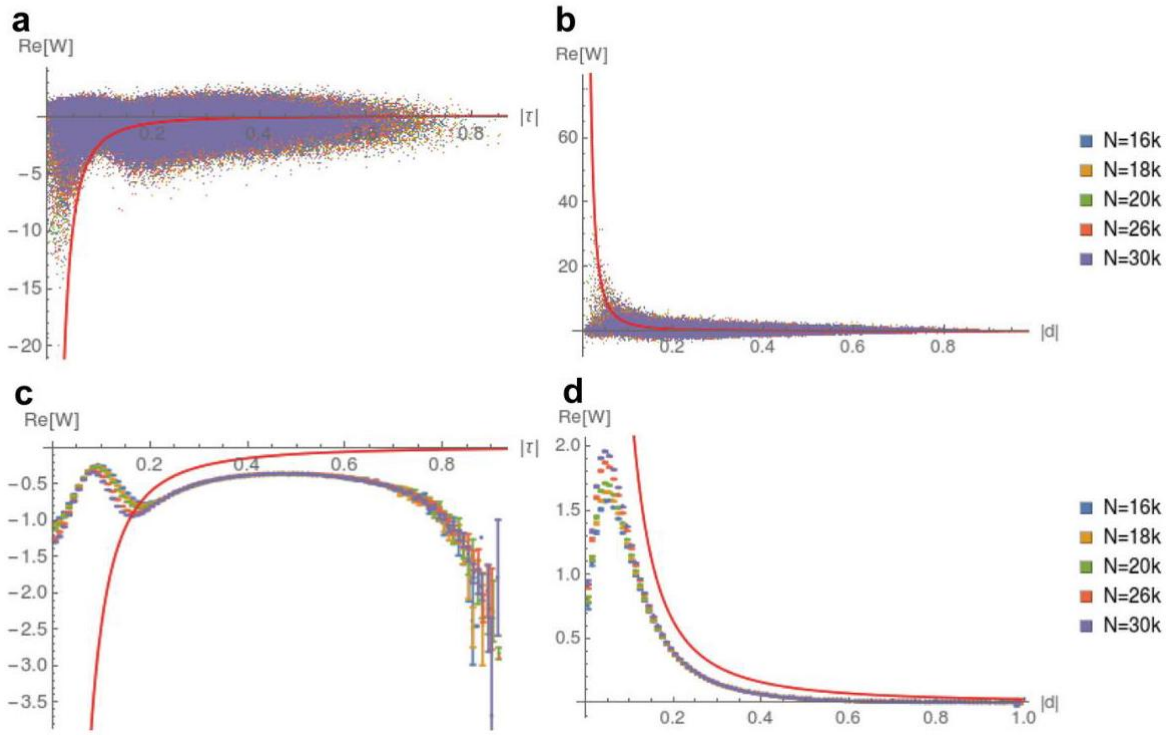

Fig. 6 (a)-(b) represent Re $[W_{SJ}]$ vs. geodesic distance for a sample of 100000 randomly selected pairs, in the 4d causal diamond; $m = 0$. (c)-(d) are plots of the binned and averaged data with the SEM. In both cases, the continuum Minkowski Wightman function Eq. (53) is shown in red. (a) Causal. (b) Spacelike. (c) Causal.

(d) Spacelike

图 6(a)-(b) 是四维因果菱形中随机抽取的 100000 对样本的 $\mathrm{Re}\,[W_{\mathrm{SJ}}]$ 随测地线距离的变化图；$m = 0$ 。(c)-(d) 是分组平均后带标准误的图。两种情况中，连续闵氏空间怀特曼函数即式 (53) 均以红色标出。(a) 因果型；(b) 类空型；(c) 因果型；(d) 类空型

In Fig. 6 we show the scatter and binned plots for $\mathrm{Re}\,[W_{\mathrm{SJ}}]$ as N are varied. The convergence with increasing density suggests that the larger N values are approaching the asymptotic regime. The Minkowski two-point function Eq. (53) is also included in this plot, and it clearly does not agree with W_{SJ} in the full diamond. The small distance behavior shows departure from the continuum, softening the divergences.

图 6 给出了改变 N 时 $\mathrm{Re}\,[W_{\mathrm{SJ}}]$ 的散点图与分组图。随着密度增加的收敛趋势表明，更大的 N 值正在趋近渐近区域。图中也给出了闵氏两点关联函数即式 (53)，显然它与整个菱形中的 W_{SJ} 并不一致。小距离行为已经偏离连续谱，软化了发散。

Figure 7 shows the scatter and binned plots for a smaller causal diamond of side length 1/2 compared to the larger diamond it is in the center of. Although the agreement of W_{SJ} with W_{mink} is not as good as in 2 d , we see that as N increases, there is a convergence of W_{SJ} to W_{mink} . This suggests that as in 2d, the 4d diamond also shows an agreement with the Minkowski vacuum far away from the boundary.

图 7 展示了位于大菱形中心、边长为 1/2 的更小因果菱形的散点图与分组图。虽然 W_{SJ} 与 W_{mink} 的契合度不如 2 d 中的情况，但我们可以看到，随着 N 增大，W_{SJ} 收敛于 W_{mink} 。这说明和二维的情况一样，四维菱形在远离边界的区域也符合闵氏真空。

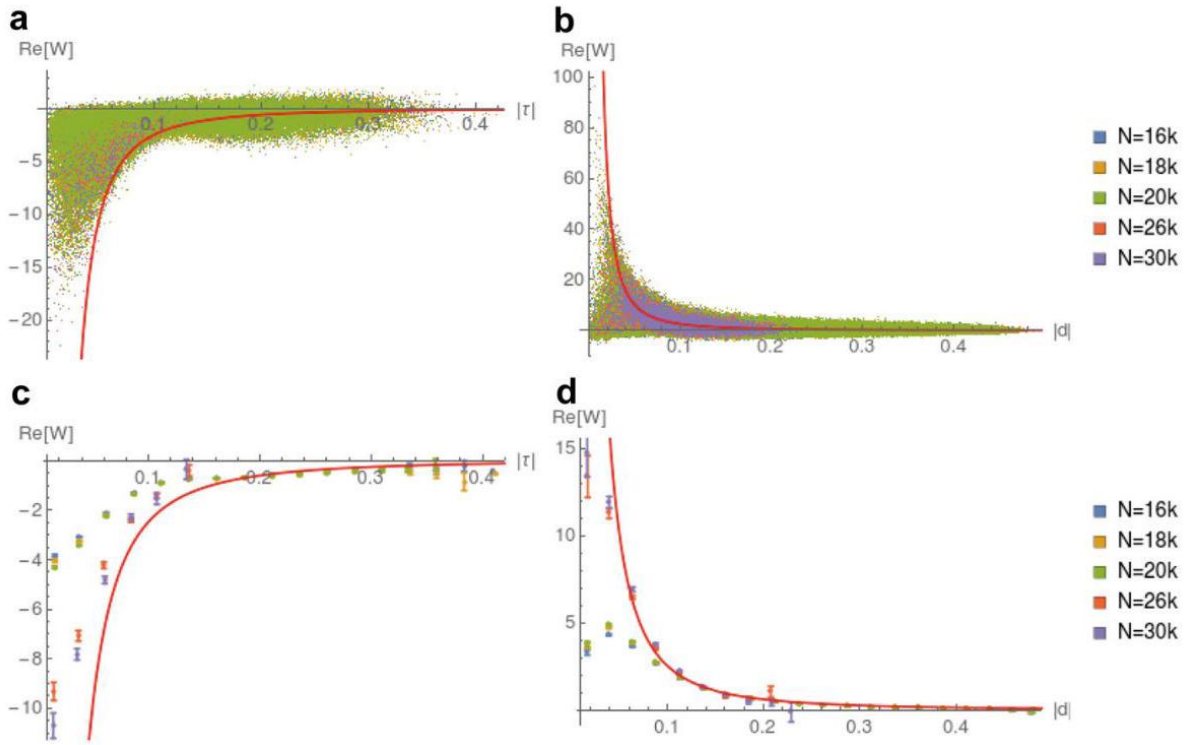

Fig. 7 (a)-(b) represent $\mathrm{Re}\left[W_{\mathrm{SJ}}\right]$ vs. geodesic distance for all pairs within a sub-diamond with height 1/2 of the full diamond, in the 4 d causal diamond; $m=0$. (c)-(d) are plots of the binned and averaged data with the SEM. In both cases, the continuum Minkowski Wightman function Eq. (53) is also shown. (a) Causal. (b) Spacelike. (c) Causal. (d) Spacelike

图 7(a)-(b) 是 4 d 维因果菱形中，完整菱形里高度为 1/2 的子菱形内部所有点对的 $\mathrm{Re}\left[W_{\mathrm{SJ}}\right]$ 随测地线距离的变化图；$m=0$ 。(c)-(d) 是分组平均后带标准误的图。两种情况中也都给出了连续闵氏空间怀特曼函数即式 (53)。(a) 因果型；(b) 类空型；(c) 因果型；(d) 类空型

Slab in dS^2

dS^2 中的板条区域

The slab we consider in de Sitter spacetime lies within the region $[-T,T]$ (T is the cutoff in the conformal time.). We also need to check convergence with T at fixed ρ , to show that the results are independent of the IR cutoff.

我们在德西特时空研究的板条区域位于 $[-T,T]$ (T 区间内 ($[-T,T]$ (T 是共形时间的截断)。我们还需要检验固定 ρ 时对 T 的收敛性，以证明结果与红外截断无关。

The Wightman function for the Euclidean vacuum in d spacetime dimensions is given by (The expression for W_E in equation $B.36$ of [3] has a minor typographical error: the factor of 4π should be raised to the power of $d/2$. See, for example,[7].)

d 维时空中欧几里得真空的怀特曼函数由下式给出 (文献 [3] 的第 $B.36$ 式中，W_E 的表达式存在一处微小排版错误: 因子 4π 应取 $d/2$ 次幂。参见例如文献 [7]。)

$$W_E(x,y)=\frac{\Gamma[h_+]\Gamma[h_-]}{(4\pi)^{d/2}\ell^2\Gamma\left[\frac{d}{2}\right]}{}_2F_1\left(h_+,h_-,\frac{d}{2};\frac{1+Z(x,y)+i\varepsilon\,\mathrm{sign}\left(x^0-y^0\right)}{2}\right),$$

(54)

where $Z(x,y)$ is related to the geodesic distance, $h_\pm=\frac{d-1}{2}\pm\upsilon,\upsilon=\ell\sqrt{m_*^2-m^2}$, $m_*=\frac{d-1}{2\ell}$ and ${}_2F_1(a,b,c;z)$ is a hypergeometric function. The symmetric two-point function, or Hadamard function, for any other Allen-Mottola α -vacuum is [3]

其中 $Z(x,y)$ 与测地线距离相关，$h_\pm=\frac{d-1}{2}\pm\upsilon,\upsilon=\ell\sqrt{m_*^2-m^2}$ 、$m_*=\frac{d-1}{2\ell}$ 和 ${}_2F_1(a,b,c;z)$ 是超几何函数。任意其他艾伦-莫托拉 α 真空的对称两点函数 (即阿达马函数) 为 [3]

$$H_{\alpha\beta}(x,x')=\cosh 2\alpha H_E(x,x')+\sinh 2\alpha\left[\cos\beta H_E(\bar{x},x')-\sin\beta\Delta(\bar{x},x')\right],$$

(55)where $\bar{x}$ is the antipodal point of x . The Wightman function is related to H by $2W=H+i\Delta$. We show comparisons with the α -vacua found to correspond to the SJ vacuum in [3]. Since we work in even dimensions, these are $\alpha=0$ for $m\geq m_*$ (yielding the Euclidean vacuum), and

其中 $\bar{x}$ 是 x 的对径点。怀特曼函数通过 $2W = H + i\Delta$ 与 H 相关联。我们将结果与文献 [3] 中被认为对应 SJ 真空的 α 真空进行对比。由于我们在偶数维中计算，当 $m \geq m_*$ 时这些真空为 $\alpha = 0$，对应欧几里得真空，即

$$\alpha = \frac{1}{2}\tanh^{-1}|\sin \pi\upsilon| \quad \text{and} \quad \beta = \pi\left[\frac{d}{2} + \theta(-\sin \pi\upsilon)\right] \tag{56}$$

for $m < m_*$.

当 $m < m_*$ 时。

We begin with 2 d de Sitter spacetime, and work in units in which the de Sitter radius $\ell = 1$. In 2 d, $m_* = 0.5$, and the conformal mass $m_c = 0$. Hence, the minimally coupled and the conformally coupled massless cases coincide. The simulations span slabs of different T values from 1 to 1.5, while N values range from $8k$ to $36k$. We show the log-log plots of the PJ spectrum for the massless $m = 0$ and for the massive (This is an arbitrary choice of mass with no special physical significance. It allows for comparisons with [3] in their 2d de Sitter causal set simulations.) $m = 2.3$ cases in Fig. 8. The spectrum converges well for both masses, with the knee shifting to the UV as N increases, as expected. We also show the comparison between the causal set spectrum with the finite T continuum spectrum obtained via the mode comparison method in [3]. As shown in Fig. 8, this spectrum does not seem to agree with the causal set spectrum even though the latter convergences with N .

我们从 2 d 维德西特时空开始研究，采用德西特半径 $\ell = 1$ 为单位。在 2 d, $m_* = 0.5$ 中，共形质量为 $m_c = 0$，因此最小耦合和共形耦合的无质量情况等价。模拟覆盖了不同 T 值的板条区域，T 取值范围为 1 到 1.5，N 的取值范围则从 $8k$ 到 $36k$ 。我们在图 8 中给出了无质量 $m = 0$ 和有质量 (这是任意选取的质量，没有特殊物理意义，仅用于和文献 [3] 的二维德西特因果集模拟结果对比) $m = 2.3$ 情况的 PJ 谱双对数图。两种质量的谱都收敛良好，如预期一般，拐点随 N 增大向紫外方向移动。我们还对比了因果集谱与文献 [3] 中通过模比较法得到的有限 T 连续谱。如图 8 所示，尽管因果集谱随 N 收敛，二者似乎并不一致。

We show W_{SJ} for both the above masses: $m = 0$ and $m = 2.3$, and vary over both the slab height T and density ρ . For $m = 2.3$, as can be seen in the scatter plots of Figs. 9,10, and 11, W_{SJ} agrees very well with the SJ vacuum expected from the calculation in [3] (the Euclidean vacuum). Furthermore, it appears that W_{SJ} for a given T is simply the restriction of W_{SJ} for a larger T . This is also in agreement with [3].

我们给出了上述两种质量 $m = 0$ 和 $m = 2.3$ 对应的 W_{SJ}，同时改变板条高度 T 和密度 ρ 。对于 $m = 2.3$，从图 9、图 10 的散点图可以看出，11, W_{SJ} 与文献 [3] 计算预期的 SJ 真空 (即欧几里得真空) 符合得非常好。此外，对于给定板条高度 T 得到的 W_{SJ}，看起来就是更大 T 对应的 W_{SJ} 的限制，这也与文献 [3] 的结论一致。

For the massless case, the @scatter plots of W_{SJ} in Figs. 12,13, and 14 do not show convergence, but instead fan out, as a function of the proper time and distance. As the density decreases, for $T = 1.56, N = 36k$, the scatter plot Fig. 14 shows a clustering into two distinct sets. This suggests that W_{SJ} may not just be a function of just proper time and distance, and hence may not be de Sitter invariant.

无质量情形下，图 12、13 和 14 中 W_{SJ} 的散点图并未展现出收敛性，反而随固有时间和距离呈发散状。当密度降低时，对于 $T=1.56, N=36k$ ，图 14 的散点图显示点聚集成两个不同集合。这表明 W_{SJ} 可能不只是固有时间和距离的函数，因此可能不满足德西特不变性。

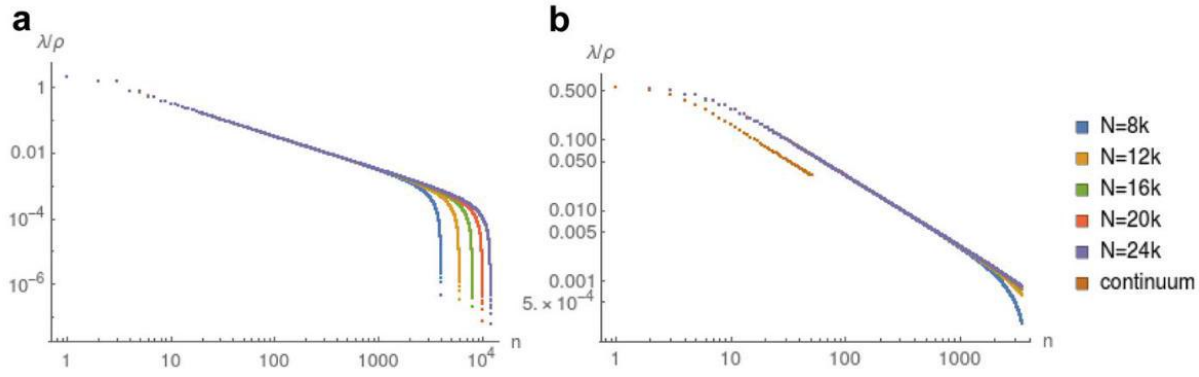

Fig. 8 Log-log plot of the positive eigenvalues of $i\Delta$ at $T=1$, in 2 d de Sitter. In the massive case on the right, we plot the largest 3500 positive eigenvalues and the corresponding continuum eigenvalues from the finite T mode comparison results of [3]. (a) $m=0$. (b) $m=2.3$

图 8 $i\Delta$ 在 $T=1$ 处、2 d 维德西特空间中正特征值的双对数图。右图为有质量情形，我们绘制了最大的 3500 个正特征值，以及文献 [3] 有限 T 模比较结果中对应的连续谱特征值。(a) $m=0$ 。(b) $m=2.3$

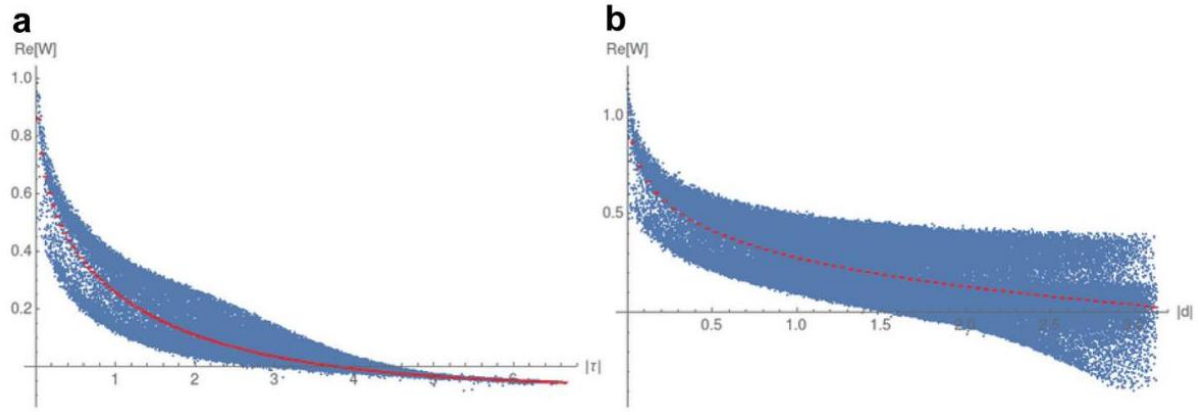

Fig. $9 N=24000, T=1, \rho=1226.31$, in 2 d de Sitter. The scatter plot is $\mathrm{Re}\left[W_{\mathrm{SJ}}\right]$ vs. geodesic distance for a sample of 100000 randomly selected pairs. The red curve represents the continuum W_E from Eq. (54). (a) Causal $m=2.3$. (b) Spacelike $m=2.3$

图 $9 N=24000, T=1, \rho=1226.31$ ， 2 d 维德西特空间中。该散点图是对随机抽取的 100000 个点对绘制的 $\mathrm{Re}\left[W_{\mathrm{SJ}}\right]$ 对测地线距离。红色曲线代表式 (54) 给出的连续谱 W_E 。(a) 类时 $m=2.3$ 。(b) 类空 $m=2.3$

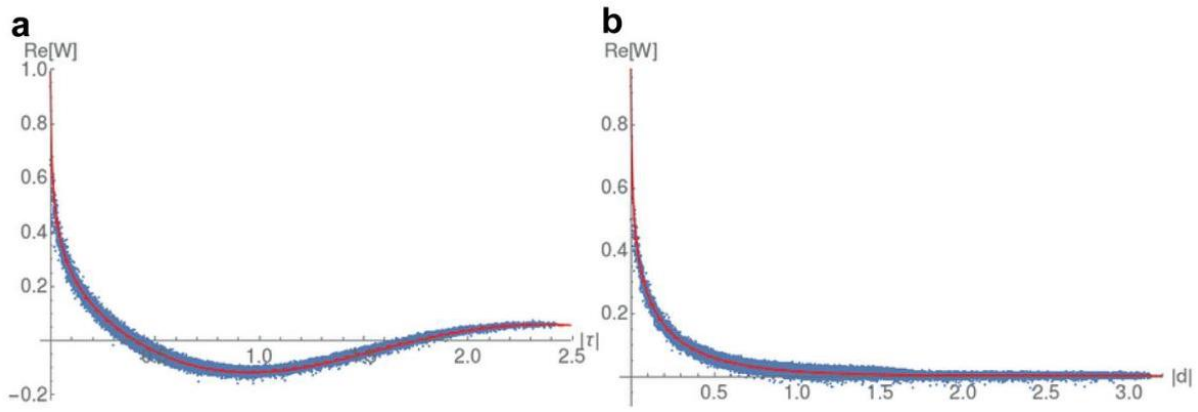

Fig. $10 N=36000, T=1.5, \rho=203.15$, in 2 d de Sitter. $\mathrm{Re}\left[W_{\mathrm{SJ}}\right]$ vs. geodesic distance for 100000 randomly selected pairs. The red curve represents the continuum W_E from Eq. (54). (a) Causal $m=2.3$. (b) Spacelike $m=2.3$

图 $10 N=36000, T=1.5, \rho=203.15$ ， 2 d 维德西特空间中。100000 个随机抽取点对的 $\mathrm{Re}\left[W_{\mathrm{SJ}}\right]$ 对测地线距离。红色曲线代表式 (54) 给出的连续谱 W_E 。(a) 类时 $m=2.3$ 。(b) 类空 $m=2.3$

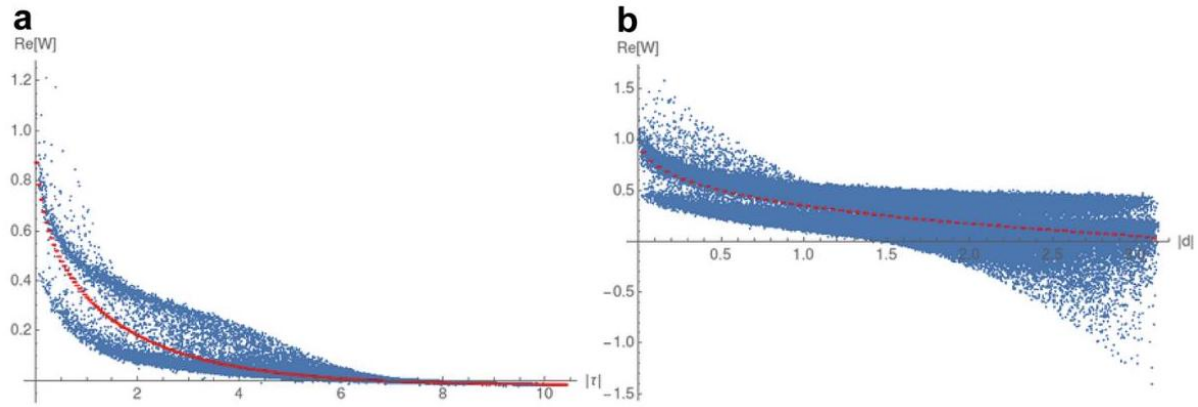

Fig. $11 N=36000, T=1.56, \rho=30.93$, in 2 d de Sitter. $\mathrm{Re}\left[W_{\mathrm{SJ}}\right]$ vs. geodesic distance for a sample of 100000 randomly selected pairs. The red curve represents the continuum W_E from Eq. (54). (a) Causal $m=2.3$. (b) Spacelike $m=2.3$

图 $11 N=36000, T=1.56, \rho=30.93$ ， 2 d 维德西特空间中。该散点图是对随机抽取的 100000 个点对绘制的 $\mathrm{Re}\left[W_{\mathrm{SJ}}\right]$ 对测地线距离。红色曲线代表式 (54) 给出的连续谱 W_E 。(a) 类时 $m=2.3$ 。(b) 类空 $m=2.3$

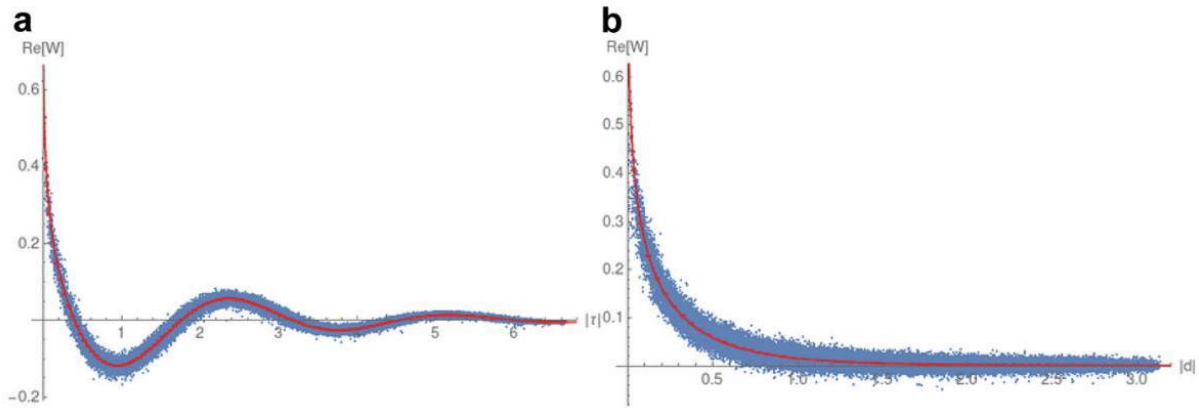

Fig. 12 $N = 32000, T = 1, \rho = 1635.08$, in 2d de Sitter. (a)-(b) represent $\mathrm{Re}\,[W_{\mathrm{SJ}}]$ vs. geodesic distance for a sample of 100000 randomly selected pairs, and the red curve represents the mean values with the SEM. (a) Causal $m = 0$. (b) Spacelike $m = 0$

图 12 $N = 32000, T = 1, \rho = 1635.08$ ， 二维德西特空间中。(a)-(b) 为随机抽取的 100000 个点对的 $\mathrm{Re}\,[W_{\mathrm{SJ}}]$ 对测地线距离，红色曲线代表带标准误的均值。(a) 类时 $m = 0$ 。(b) 类空 $m = 0$

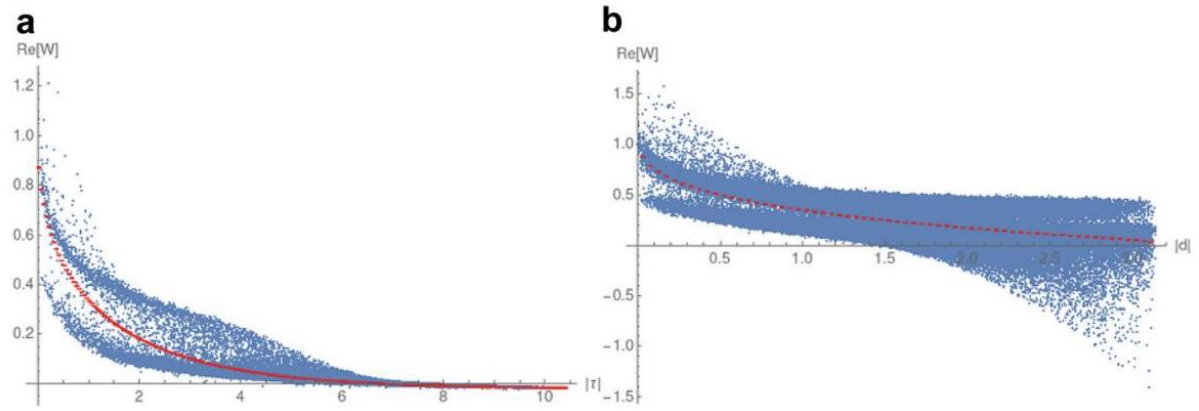

Fig. 13$N = 36000, T = 1.5, \rho = 203.15$, in 2 d de Sitter. (a)-(b) represent $\mathrm{Re}\,[W_{\mathrm{SJ}}]$ vs. geodesic distance for a sample of 100000 randomly selected pairs. The red curve represents the mean values with the SEM. (a) Causal $m = 0$. (b) Spacelike $m = 0$

图 13$N = 36000, T = 1.5, \rho = 203.15$ ， 2 d 维德西特空间中。(a)-(b) 为随机抽取的 100000 个点对的 $\mathrm{Re}\,[W_{\mathrm{SJ}}]$ 对测地线距离。红色曲线代表带标准误的均值。(a) 类时 $m = 0$ 。(b) 类空 $m = 0$

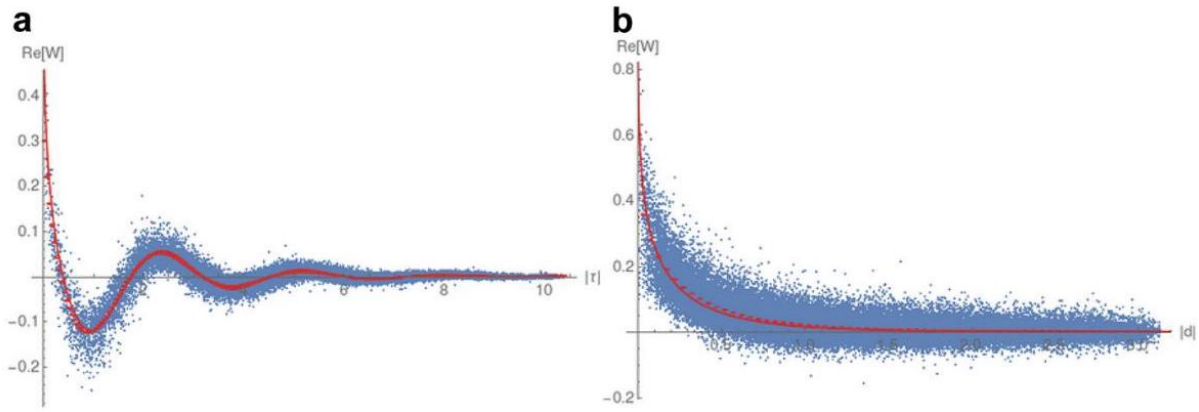

Fig. 14$N = 36000, -1.56 < \widetilde{T} < 1.56, \rho = 30.93$, in 2 d de Sitter. (a)-(b) represent Re $[W_{\rm SJ}]$ vs. geodesic distance for a sample of 100000 randomly selected pairs. The red curve represents the mean values with the SEM. (a) Causal $m = 0$. (b) Spacelike $m = 0$

图 14$N = 36000, -1.56 < \widetilde{T} < 1.56, \rho = 30.93$ ，位于 2 d 德西特空间中。(a)-(b) 展示了 100000 对随机选取样本的 Re $[W_{\rm SJ}]$ 与测地线距离的关系。红色曲线表示带标准误的平均值。(a) 类光因果 $m = 0$ 。(b) 类空 $m = 0$

Slab in dS^4

dS^4 中的板区域

Finally, we present simulations for the 4 d de Sitter SJ vacuum. In 4 d, $m_* = 1.5$ and $m_c = \sqrt{2} \approx 1.41$.

最后，我们展示了 4 d 德西特空间中索金-约翰斯顿真空的模拟结果，详见 4 d, $m_* = 1.5$ 和 $m_c = \sqrt{2} \approx 1.41$ 。

Figure 15 shows the log-log plot of the SJ spectrum for $m = 0$ and $m = 2.3$ for various N . We find excellent convergence with N in both cases, and again, as in the other cases, there is a knee which shifts to the UV as N is increased. However, there is poor agreement with the continuum values of the finite T spectrum calculated via the mode comparison method in [3], as in the 2d case. There is also no unusual behavior close to the masses $m = 0$ and $m = m_c \approx 1.41$ [28].

图 15 给出了不同 N 下，$m = 0$ 和 $m = 2.3$ 的索金-约翰斯顿谱双对数图。我们发现两种情况下，谱随 N 都收敛得很好；并且和其他情形一样，谱存在一个拐点，当 N 增大时，拐点向紫外方向移动。然而和二维情形一样，我们的结果与文献 [3] 中通过模比较法计算得到的有限 T 谱的连续值一致性很差。在质量为 $m = 0$ 和 $m = m_c \approx 1.41$ 附近也没有出现异常行为 [28]。

Figures 16 and 17 are sample scatter plots of $W_{\rm SJ}$ for $m = 0$ and $m = 2.3$. In Fig. 18 we fix T for $m = 0$ and for $m = m_c \approx 1.41$ and vary N to check for convergence with density; for smaller proper times and distances, the convergence is not as good as it is for larger proper times and distances. For $m = 1.41$ we also plot the Wightman function associated with the Euclidean vacuum W_E in Eq. (54). W_E does not compare well with the causal set $W_{\rm SJ}$. The convergence with T can also be checked and is good for various m values.

However, the Wightman function associated with the α -vacuum Eq. (55) as well as the Euclidean vacuum W_E once again does not compare well with the causal set W_{SJ} for any of these masses. Overall, simulations strongly suggest that the causal set 4 d de Sitter W_{SJ} differs from the Mottola-Allen α -vacua for all masses. In particular, there is modification of the small distance behavior of the state, making it well-defined in the UV limit.

图 16 和图 17 是 W_{SJ} 分别在 $m=0$ 和 $m=2.3$ 情况下的样本散点图。在图 18 中，我们固定 $m=0$ 和 $m=m_c\approx 1.41$ 对应的 T ，改变 N 来检验随密度的收敛性；对于较小的固有时和距离，收敛效果不如更大的固有时和距离的情况。对于 $m=1.41$ ，我们还绘制了与欧几里得真空 W_E 相关的怀特曼函数，见式 (54)。W_E 和因果集 W_{SJ} 的吻合度很差。我们也检验了随 T 的收敛性，对于不同的 m 值收敛效果都很好。然而，与式 (55) 中 α 真空相关的怀特曼函数以及欧几里得真空 W_E ，对于任意质量都再次和因果集 W_{SJ} 吻合度很差。整体来看，模拟结果强烈表明，因果集 4 d 德西特空间的 W_{SJ} 与所有质量下的莫托拉-艾伦 α 真空都不相同。特别地，该态小距离行为发生了改变，使得它在紫外极限下是良好定义的。

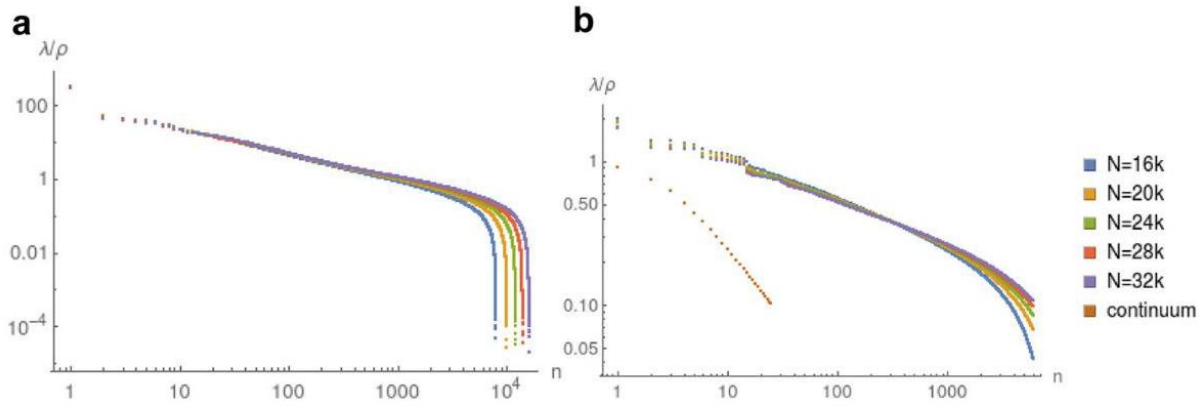

Fig. 15 Log-log plot of the positive eigenvalues of $i\Delta$, in 4d de Sitter. In the massive case on the right, we plot the largest 6000 positive eigenvalues and the corresponding continuum eigenvalues from the finite T mode comparison results of [3]. (a) $m=0$. (b) $m=2.3$

图 15 四维德西特空间中 $i\Delta$ 正特征值的双对数图。右图为有质量情形，我们绘制了最大的 6000 个正特征值，以及文献 [3] 中有限 T 模比较结果得到的对应连续特征值。(a) $m=0$ 。(b) $m=2.3$

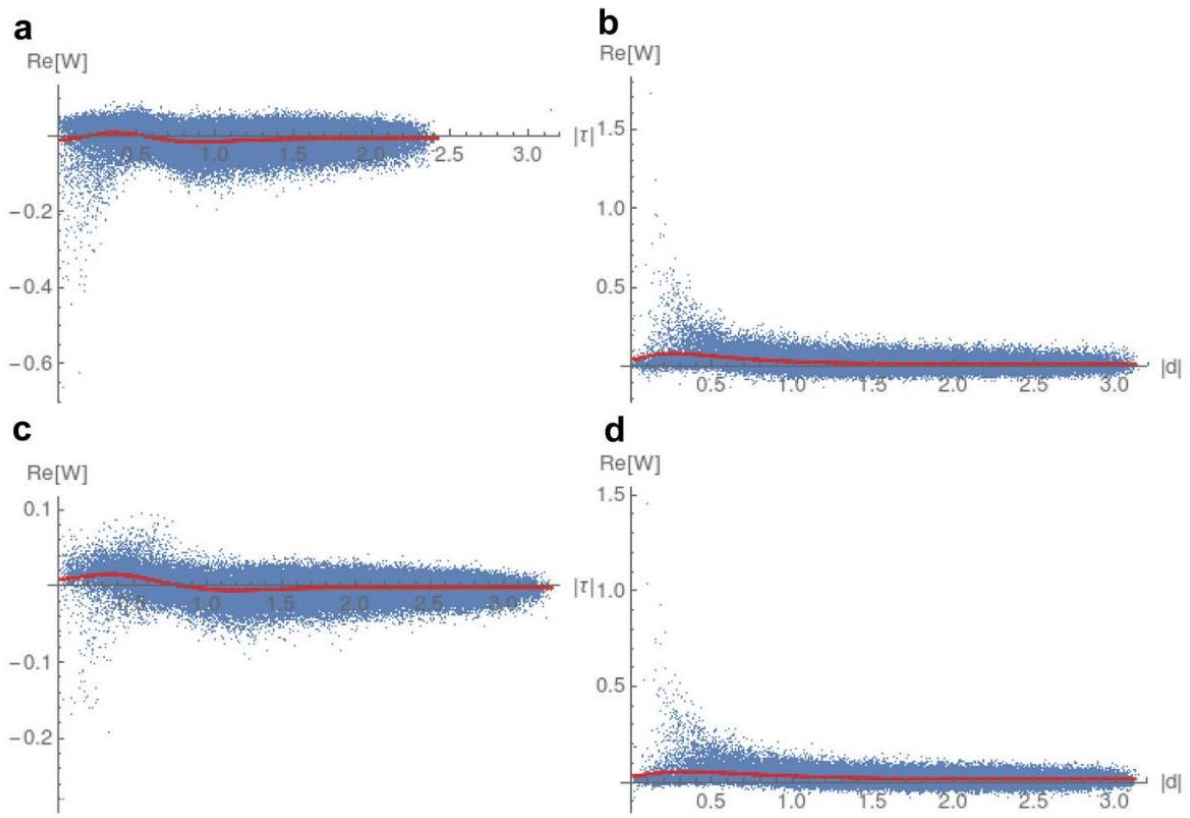

Fig. $16 m=0, N=32000$, in 4d de Sitter. $\mathrm{Re}\left[W_{\mathrm{SJ}}\right]$ vs. geodesic distance for 100000 randomly selected pairs, and the red curve represents the mean values with the SEM. (a) Causal $T=1$. (b) Spacelike $T=1$. (c) Causal $T=1.2$. (d) Spacelike $T=1.2$

图 $16 m=0, N=32000$ ，四维德西特空间中。$\mathrm{Re}\left[W_{\mathrm{SJ}}\right]$ 随测地线距离的变化，数据来自随机选取的 100000 对点，红色曲线代表带标准误的均值。(a) 因果类 $T=1$ 。(b) 类空 $T=1$ 。(c) 因果类 $T=1.2$ 。(d) 类空 $T=1.2$

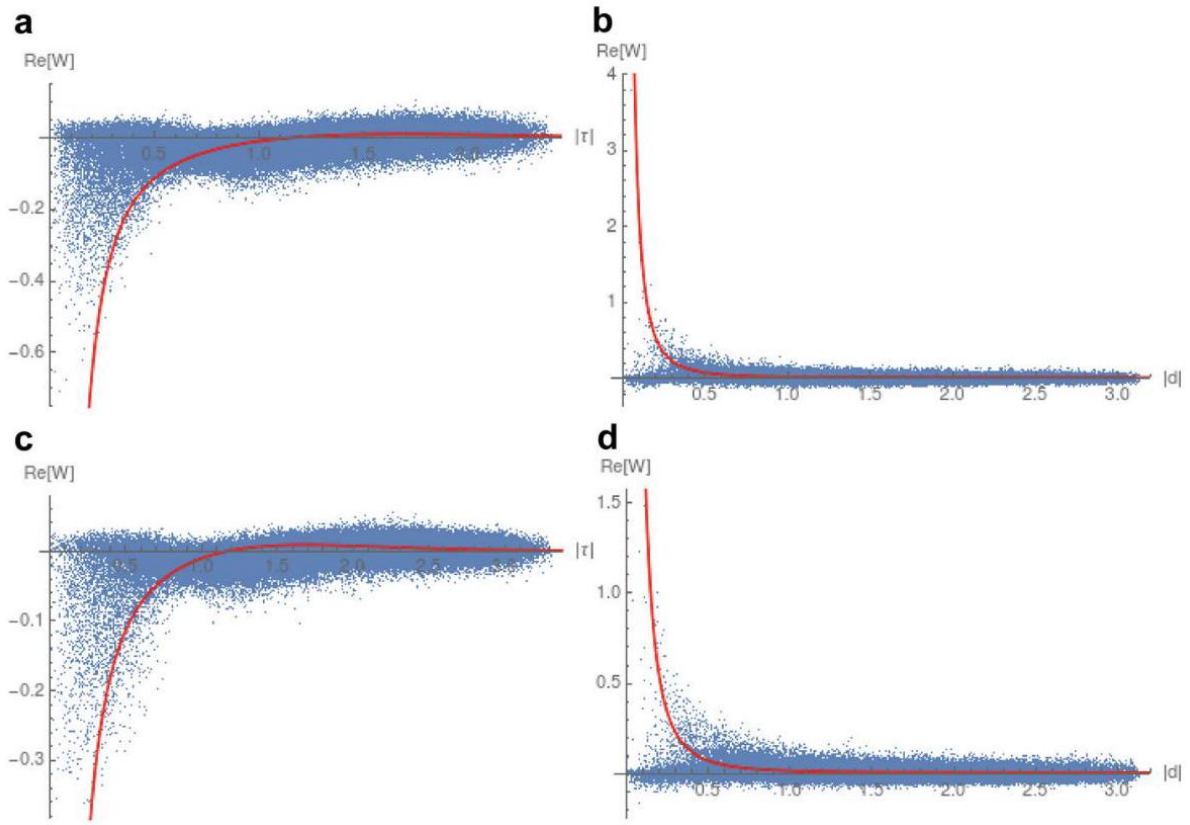

Fig. 17 $m = 2.3, N = 32000$, in 4 d de Sitter. $\mathrm{Re}\,[W_{\mathrm{SJ}}]$ vs. geodesic distance for a sample of 100000 randomly selected pairs. The red curve shows the Euclidean two-point function W_E from Eq. (54). (a) Causal $T = 1$. (b) Spacelike $T = 1$. (c) Causal $T = 1.2$. (d) Spacelike $T = 1.2$

图 17 $m = 2.3, N = 32000$ ，4 d 维德西特空间中。$\mathrm{Re}\,[W_{\mathrm{SJ}}]$ 随测地线距离的变化，数据来自随机选取的 100000 对点样本。红色曲线为式 (54) 中的欧几里得两点关联函数 W_E 。(a) 因果类 $T = 1$ 。(b) 类空 $T = 1$ 。(c) 因果类 $T = 1.2$ 。(d) 类空 $T = 1.2$

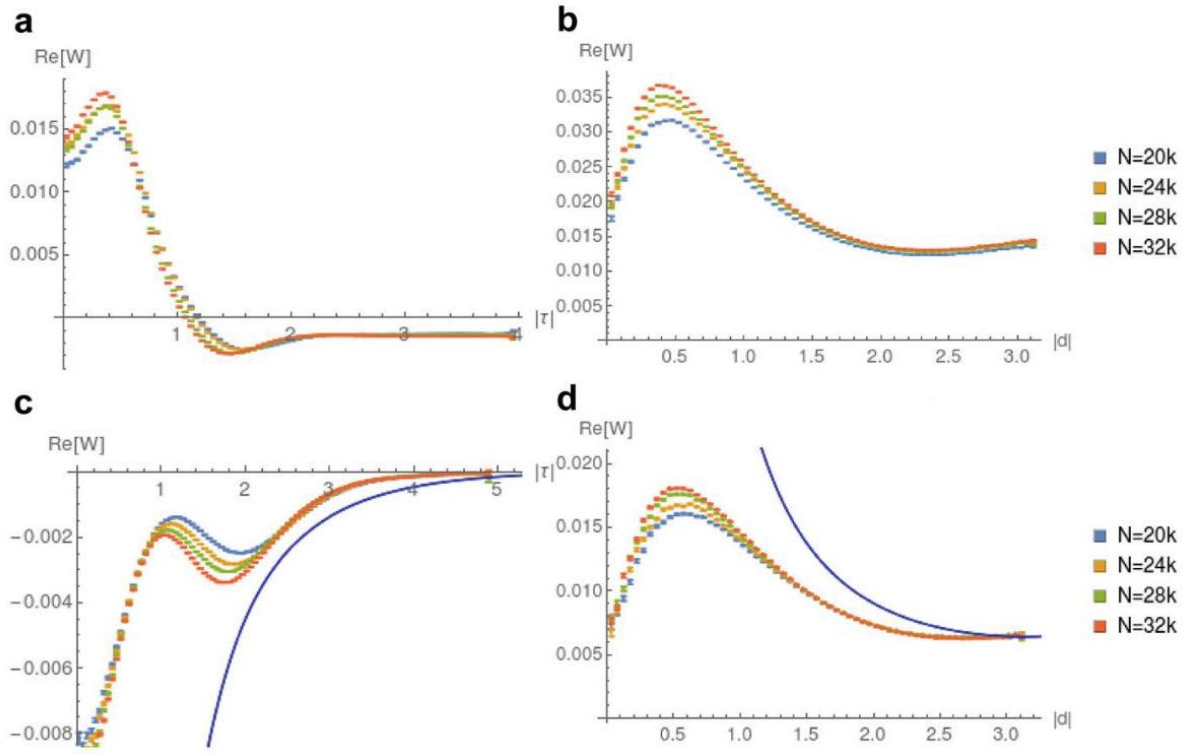

Fig. 18 Re $[W_{\mathrm{SJ}}]$ vs. geodesic distance with varying density, in 4 d de Sitter. The blue curve shows the Euclidean two-point function as a reference. (a) Causal $m = 0, T = 1.3$. (b) Spacelike $m = \ 0, T = 1.3$. (c) Causal $m = 1.41, T = 1.4$. (d) Spacelike $m = 1.41, T = 1.4$

图 18 在 4 d 德西特空间中，Re $[W_{\mathrm{SJ}}]$ 随测地线距离在不同密度下的变化关系。蓝色曲线为欧几里得两点函数，用作参考。(a) 因果 $m = 0, T = 1.3$ 。(b) 类空 $m = \ 0, T = 1.3$ 。(c) 因果 $m = 1.41, T = 1.4$ 。(d) 类空 $m = 1.41, T = 1.4$

Concluding Remarks

结束语

Before concluding, we mention two ideas that have been explored around building a QFT on causal sets:

在总结之前，我们介绍两个围绕因果集上构建量子场论已经探索过的思路:

- Equations of motion: This arises as an aside to the SJ construction is the causal set - namely looking at time evolution as a set of algebraic constraints on the field configuration rather than a discretized differential operator (i.e., the d'Alembertian). Such constraints can be obtained from the relation:

- 运动方程: 这是作为因果集 SJ 构造的附带问题产生的——即把时间演化看作场构形上的一组代数约束，而非离散化微分算符 (也就是达朗贝尔算符)。这类约束可以由下述关系得到:

$$\mathrm{Ker}\left(\widehat{\Box}-m_p^2\right)=\overline{\mathrm{Im}\left(\widehat{\Delta}\right)}.$$

In principle this is applicable to a globally hyperbolic region of any general spacetime.

原则上，它适用于任意一般时空的整体双曲区域。

On the causal set, a solution of the field equation $b \in \mathrm{Ker}\left(\widehat{\Box}\right)$ also lies in $\mathrm{Im}\left(\widehat{\Delta}\right)$; therefore (We use indices here instead of coordinates to emphasize that the objects here are matrices.),

在因果集上，场方程 $b \in \mathrm{Ker}\left(\widehat{\Box}\right)$ 的解也属于 $\mathrm{Im}\left(\widehat{\Delta}\right)$ ； 因此 (我们在此用指标而非坐标来强调这里的对象都是矩阵),

$$b_x=\sum_{k=1}^{r} a_k s_{kx} \tag{57}$$

where s_{kx} span $\mathrm{Im}\left(\widehat{\Delta}\right)$ are just the SJ modes and $r=\dim\left(\mathrm{Im}\left(\widehat{\Delta}\right)\right)$. We can think of this equation as an initial value problem by assigning known values to some "initial points" in the causal set, i.e., some values in the solution vector b can be assigned as initial values. A preliminary discussion on this can be found in [21].

其中 s_{kx} 、$\mathrm{Im}\left(\widehat{\Delta}\right)$ 就是 SJ 模，$r=\dim\left(\mathrm{Im}\left(\widehat{\Delta}\right)\right)$ 。我们可以把这个方程看作初值问题: 给因果集中的若干“初始点”赋予已知值，也就是解向量 b 中的部分值可以指定为初值。相关的初步讨论可见文献 [21]。

- Fermions: To discuss QFT for fermions, we need a way to first obtain the retarded Green function analogue on the causal set and then use an appropriate PJ operator in order to get a unique set of modes. The latter issue is resolved easily by replacing the bosonic PJ operator, which is written as a commutator of field operators, with a fermionic version based on an anti-commutator, i.e.,

- 费米子: 要讨论费米子的量子场论，我们需要先得到因果集上推迟格林函数的对应构造，再使用合适的 PJ 算符来得到唯一一组模。后者很容易解决: 原本玻色子 PJ 算符写作场算符的对易子，我们只需将其替换为基于反对易子的费米子版本，即:

$$\left\{\widehat{\phi}_\alpha(x),\widehat{\phi}_\beta(y)^\dagger\right\}=i\Delta_{\alpha,\beta}(x,y).$$

Here α,β are spin indices.

此处 α,β 是自旋指标。

In [19], Johnston gives two proposals for constructing spin-1/2 Green functions on the causal set. The first one uses the Feynman checkerboard idea [14] which involves a path sum involving paths that zigzag in spacetime and are made up of null geodesics. The second one uses the notion that the Green function for the Dirac equation can be constructed as a "square root" of the Klein-Gordon Green function. The main insight here is that if we define

在文献 [19] 中，Johnston 给出了在因果集上构造自旋 1/2 格林函数的两个方案。第一个使用费曼棋盘思路 [14]，该思路需要对由类光测地线组成、在时空中之字形行进的路径进行求和。第二个方案基于这样一个概念: 狄拉克方程的格林函数可以构造为克莱因-戈登格林函数的“平方根”。其核心见解是，如果我们定义

$$S_m(x-y) \equiv -\int d^d z R_m(x-z) R_{-m}(z-y)$$

such that R satisfies the Dirac equation, then S satisfies the Klein-Gordon equation. Like in the bosonic case, we can use a series expansion to get R_m once R_0 is determined. A similar construction can be used on causal sets. However, the square root of a matrix (if it exists) is not unique in general, and therefore we may need further constraints.

使得 R 满足狄拉克方程，那么 S 就满足克莱因-戈登方程。和玻色子的情况一样，确定 R_0 后我们可以通过级数展开得到 R_m 。因果集上也可以使用类似的构造。但矩阵的平方根 (即使存在) 一般不是唯一的，因此我们可能需要额外的约束条件。

QFT on causal sets is an important direction in the broad area of computational (numerical) QFT and in discrete approaches to quantum gravity. While we are not working here in the deep UV regime of full quantum gravity, we are working at a mesoscale where the effects of discreteness are still relevant to the dynamics of the quantum field. We showed how a free scalar field theory can be set up in various situations through the use of the SJ method. We also mentioned other proposals around describing matter on a causal set. Such studies still have a long way to go. Firstly, there are conceptual implications of defining such a state - we mentioned that the SJ state coincides with the usual vacuum in static spacetimes. This is a limited result, and it is not always clear how the SJ state corresponds to other states that can be defined in general spacetimes. Mathematically, this is a consequence of working with finite regions, while other standard states are usually defined in full spacetime. The answer to the question - ”the SJ state is the natural state for which observer?” - is not obvious. Secondly, we would like to apply this construction to more realistic theories - interacting theories and theories involving fermions. The true test of utility and of phenomenological relevance has to come from S-matrix calculations for these theories. Some exciting ideas have been proposed in these directions [16, 19], and these need to be pushed further in order to deepen our understanding of the propagation of quantum fields on causal sets.

因果集上的量子场论是计算 (数值) 量子场论以及量子引力离散方法领域中一个重要的研究方向。我们的研究并不涉及完整量子引力的深紫外区，而是工作在介观尺度——在该尺度离散性效应仍对量子场的动力学有影响。我们展示了如何通过 SJ 方法在多种场景下构建自由标量场理论，也介绍了描述因果集上物质的其他方案。这类研究仍有很长的路要走。首先，定义这样的状态存在概念层面的问题——我们提到过 SJ 态在静态时空中和普通真空一致，但这是个有限的结论，在一般时空中 SJ 态如何对应其他可定义的状态并不总是清晰的。从数学上讲，这是我们在有限区域内工作的结果，而其他标准状态通常定义在完整时空上。“SJ 态是对于哪个观测者而言的自然状态?”这个问题的答案并不明确。其次，我们希望将该构造应用到更真实的理论——相互作用理论和包含费米子的理论。这套构造是否实用、是否具有唯学相关意义，最终必须经过这些理论 S 矩阵计算的检验。目前在这些方向已经提出了许多引人关注的思路 [16, 19]，需要进一步推进，以加深我们对量子场在因果集上传播的理解。

References

参考文献

1. N. Afshordi, S. Aslanbeigi, R.D. Sorkin, A distinguished vacuum state for a quantum field in a curved spacetime: formalism, features, and cosmology. JHEP 08, 137 (2012). https://doi.org/ 10.1007/JHEP08(2012)137

2. N. Afshordi, M. Buck, F. Dowker, D. Rideout, R.D. Sorkin, Y.K. Yazdi, A ground state for the causal diamond in 2 dimensions. JHEP 10, 088 (2012). https://doi.org/10.1007/ JHEP10(2012)088

3. S. Aslanbeigi, M. Buck, A preferred ground state for the scalar field in deSitter space. JHEP 08, 039 (2013). https://doi.org/10.1007/JHEP08(2013)039

4. S. Aslanbeigi, M. Saravani, R.D. Sorkin, Generalized causal set d'alembertians. J. High Energy Phys. 2014(6) (2014). https://doi.org/10.1007/jhep06(2014)024

5. A. Aste, Resummation of mass terms in perturbative massless quantum field theory. Lett. Math. Phys. 81, 77-92 (2007). https://doi.org/10.1007/s11005-007-0169-8

6. D.M.T. Benincasa, F. Dowker, The scalar curvature of a causal set. Phys. Rev. Lett. 104, 181301 (2010). https://doi.org/10.1103/PhysRevLett.104.181301

7. R. Bousso, A. Maloney, A. Strominger, Conformal vacua and entropy in de Sitter space. Phys. Rev. D65, 104039 (2002). https://doi.org/10.1103/PhysRevD.65.104039

8. M. Brum, K. Fredenhagen, "Vacuum-like" Hadamard states for quantum fields on curved spacetimes. Class. Quant. Grav. 31, 025024 (2014). https://doi.org/10.1088/0264-9381/31/ 2/025024

9. E. Dable-Heath, C.J. Fewster, K. Rejzner, N. Woods, Algebraic classical and quantum field theory on causal sets. Phys. Rev. D 101(6), 065013 (2020). https://doi.org/10.1103/PhysRevD.101.065013

10. A.R. Daughton, The Recovery of Locality for Casual Sets and Related Topics. Ph.D. thesis, Syracuse University, 1993

11. F. Dowker, L. Glaser, Causal set d'alembertians for various dimensions. Class. Quant. Grav. 30(19), 195016 (2013)

12. C.J. Fewster, The art of the state. Int. J. Mod. Phys. D27(11), 1843007 (2018). https://doi.org/ 10.1142/S0218271818430071

13. C.J. Fewster, R. Verch, On a recent construction of "Vacuum-like" quantum field states in curved spacetime. Class. Quant. Grav. 29, 205017 (2012). https://doi.org/10.1088/0264-9381/ 29/20/205017

14. R.P. Feynman, A.R. Hibbs, D.F. Styer, Quantum Mechanics and Path Integrals (Courier Corporation, Dover Publishers, US, 2010)

15. B.Z. Foster, T. Jacobson, Quantum field theory on a growing lattice. J. High Energy Phys. 2004(08), 024-024 (2004). https://doi.org/10.1088/1126-6708/2004/08/024

16. E. Hawkins, C. Minz, K. Rejzner, Quantization, dequantization, and distinguished states (2022)

17. S. Johnston, Particle propagators on discrete spacetime. Class. Quant. Grav. 25, 202001 (2008). https://doi.org/10.1088/0264-9381/25/20/202001

18. S. Johnston, Correction terms for propagators and d'alembertians due to spacetime discreteness. Class. Quant. Grav. 32(19), 195020 (2015). https://doi.org/10.1088/0264-9381/32/19/ 195020

19. S.P. Johnston, Quantum fields on causal sets. Ph.D. thesis, Imperial College, London, 2010. http://inspirehep.net/recor

20. A. Mathur, S. Surya, Sorkin-Johnston vacuum for a massive scalar field in the 2D causal diamond. Phys. Rev. D100(4), 045007 (2019). https://doi.org/10.1103/PhysRevD.100.045007

21. X. Nomaan, Aspects of quantum fields on causal sets. Doctoral dissertation, Ph.D. thesis, Jawaharlal Nehru University, 2021

22. X. Nomaan, F. Dowker, S. Surya, Scalar field green functions on causal sets. Class. Quant. Grav. 34(12), 124002 (2017). https://doi.org/10.1088/1361-6382/aa6bc7

23. R.B. Salgado, Toward a quantum dynamics for causal sets. Syracuse University, 2008

24. R.D. Sorkin, Does locality fail at intermediate length-scales, in Approaches to Quantum Gravity: Toward a New Understanding of Space Time and Matter, ed. D. Oriti (Cambridge University Press, 2009), pp. 26-43

25. R.D. Sorkin, Scalar field theory on a causal set in histories form. J. Phys. Conf. Ser. 306, 012017 (2011). https://doi.org/10.1088/1742-6596/306/1/012017

26. R.D. Sorkin, From green function to quantum field. Int. J. Geom. Meth. Mod. Phys. 14(08), 1740007 (2017). https://doi.org/10.1142/S0219887817400072

27. R.P. Stanley, Enumerative Combinatorics, vol. 1 (Wadsworth Inc., California, 1986)

28. S. Surya, X. Nomaan, Y.K. Yazdi, Studies on the SJ vacuum in de Sitter spacetime. JHEP 07, 009 (2019). https://doi.org/10.1007/JHEP07(2019)009

29. R. Sverdlov, L. Bombelli, Gravity and matter in causal set theory. Class. Quant. Grav. 26(7), 075011 (2009)

30. R.M. Wald, Quantum Field Theory in Curved Space-Time and Black Hole Thermodynamics. Chicago Lectures in Physics (University of Chicago Press, Chicago, IL, 1995)